UNIVERZITA KARLOVA
1. lékařská fakulta

Mag. farm. Danica Michaličková, Ph.D.

Population pharmacokinetic modeling as a tool to identify covariates important for drug dosing

Populační modelování farmakokinetiky jako nástroj k identifikaci kovariát významných pro dávkování léčiv

Habilitation thesis
Habilitační prace

Field of study: Medical pharmacology
Obor: Lékařská farmakologie

Prague, 2024.
Praha, 2024.

Prohlášení:

Prohlašuji, že jsem habilitační práci zpracovala samostatně a že jsem řádně uvedla a citovala všechny použité prameny a literaturu. Současně prohlašuji, že práce nebyla využita k získání jiného nebo stejného titulu.
Souhlasím s trvalým uložením elektronické verze mé práce v databázi systému meziuniverzitního projektu Theses.cz za účelem soustavné kontroly podobnosti kvalifikačních prací.

V Praze, 31.1.2024

Danica Michaličková
Podpis:

Identifikační záznam:

Michaličková, Danica. **Population pharmacokinetic modeling as a tool to identify covariates important for drug dosing** [Populační modelování farmakokinetiky jako nástroj k indentifikaci kovariát významných pro dávkování léčiv]. Praha, 2024. 72 strany, 7 příloh. Habilitační práce. Univerzita Karlova v Praze, 1. lékařská fakulta, Farmakologický ústav.

Contents

Abbreviations

AUC = area under the curve
BSA = body surface area
BW = body weight
CI = confidence interval
CKD-EPI = Chronic Kidney Disease Epidemiology Collaboration
CL = clearance
CPB = cardiopulmonary bypass
CRP = C-reactive protein
CRRT = continuous renal replacement therapy
CWRES = conditional weighted residuals
DDI = drug-drug interactions
ECC = extracorporeal circulation
ECMO = extracorporeal membrane oxygenation
eGFR = estimated glomerular filtration rate
ESRD = end-stage renal disease
GOF = goodness-of-fit
HIE = hypoxic-ischemic encephalopathy
HF = high flux
IIV = inter-individual variability
IOV = inter-occasional variability
ISPD = international society for peritoneal dialysis
IQR = interquartile range
i.v. = intravenously
IWRES = individual weighted residuals
LD = loading dose
LF = low flux
MD = maintenance dose
MiECC = minimally invasive extracorporeal circulation
MIC = minimum inhibitory concentration
NMLE = non-linear mixed effects
NPDE = normalized prediction distribution error
OFV = objective function value
PBPK = physiologically based pharmacokinetic
PD = pharmacodynamic/pharmacodynamics
PIM = pediatric index of mortality
PK = pharmacokinetic/pharmacokinetics

PNA = postnatal age
p.o. = per os
pop = population
PTA = probability of target attainment
PWRES = population-weighted residuals
Q = intercompartmental clearance
RSE = relative standard error
RUV = residual unexplained variability
s.c. = subcutaneously
TPE = therapeutic plasma exchange
Vd = volume of distribution
UGT = uridine 5'-diphosphate-glucuronosyltransferases
VA = veno-arterial
VPC = visual predictive check
VV = veno-venous

Acknowledgements

I owe big thanks to Dr. Elke Krekels, who taught me the methods of population pharmacokinetic modelling, for the selflessness with which she shared her great knowledge and experience with me. I am greatly thankful for the useful advice, patience, and friendly approach.
I greatly thank prof. Slanar for his support, trust, always useful advice and understanding.
I thank also Dr. Pokorna, for her trust, friendly approach, and support.
I also thank my colleagues from the Institute of Pharmacology for their collaboration, and friendly environment.
Last but not least, I would like to thank my family and friends for great understanding, tremendous support, and endless patience.

List of publications

*Corresponding author

1. Michalickova, D.*, Minic, R., Dikic, N., et al. (2016). Lactobacillus helveticus Lafti L10 supplementation reduces respiratory infection duration in a cohort of elite athletes: a randomized, double-blind, placebo-controlled trial. Appl Physiol Nutr Metab 41(7), 782-789. **Q2, IF: 2.023**
2. Michalickova, D.*, Kostic-Vucicevic, M., Vukasinovic-Vesic, M., et al. (2017): Lactobacillus helveticus Lafti L10 supplementation modulates mucosal and humoral immunity in elite athletes: A randomized, double-blind, placebo-controlled trial. J Strength Cond Res 31(1), 62-70. **Q2, IF: 2.325**
3. Kostic-Vucicevic, M., Michalickova, D., Dikic, N., et al. (2018). Food elimination based on immunoglobulin G antibodies improves gastrointestinal discomfort symptoms and sport performance in professional athletes. Med Dello Sport 70(4), 480-494. **Q4, IF: 0.393**
4. Michalickova, D.*, Kotur-Stevuljevic, J., Miljkovic, M., et al. (2018). Effects of probiotic supplementation on selected parameters of blood prooxidant-antioxidant balance in elite athletes: a double-blind randomized placebo-controlled study. J Hum Kinet 64(1), 111-122. **Q3, IF: 1.414**
5. Minić, R., Papić, Z., Đorđević, B., Michaličkova, D., et al. (2018). Profiling of microorganism-binding serum antibody specificities in professional athletes. Plos One 13(9), e0203665. **Q2, IF: 2.776**
6. Michaličková, D.*, Belović, M., Ilić, N., et al. (2019). Comparison of polyphenol-enriched tomato juice and standard tomato juice for cardiovascular benefits in subjects with stage 1 hypertension: A randomized controlled study. Plant Foods Hum Nutr 74, 122-127. **Q1, IF: 2.901**
7. Michaličková, D.*, Hrnčíř, T., Canová, N. K., et al. (2020). Targeting Keap1/Nrf2/ARE signaling pathway in multiple sclerosis. Eur J Pharmacol 873, 172973. **Q2, IF: 4.432**
8. Michalicková, D.*, Pokorná, P., Tibboel, D., et al. (2020). Rapid increase in clearance of phenobarbital in neonates on extracorporeal membrane oxygenation: a pilot retrospective population pharmacokinetic analysis. Pediatr Crit Care Med 21(9), e707-e715. **Q1, IF: 3.624**
9. Michaličková, D.*, Martin, Šíma, Slanař, O. (2020). New insights in the mechanisms of impaired redox signaling and its interplay with inflammation and immunity in multiple sclerosis. Physiol Res 69.1 69(1), 1. **Q4, IF: 1.881**
10. Michalickova, D.*, Minic, R., Kotur-Stevuljevic, J., et al. (2020). Changes in parameters of oxidative stress, immunity, and behavior in endurance athletes during a preparation period in winter. J Strength Cond Res 34(10), 2965-2973. **Q2, IF: 3.781**
11. Michaličková, D.*, Jansa, P., Bursová, M., et al. (2020). Population pharmacokinetics of riociguat and its metabolite in patients with chronic thromboembolic pulmonary hypertension from routine clinical practice. Pulm Circ 10(1), 2045894019898031. **Q3, IF: 3.017**
12. Ľupták, M, Michaličková, D, Fišar, Z, et al. (2021). Novel approaches in schizophrenia-from risk factors and hypotheses to novel drug targets. World J Psychiatry 11, 7:277. **Q3, IF: 3.5**
13. Šíma, M., Michaličková, D., Slanař, O. (2021). What is the best predictor of phenobarbital pharmacokinetics to use for initial dosing in neonates? Pharmaceutics 13(3), 301. **Q1, IF: 6.525**

14. Šíma, M., Michaličková, D., Ryšánek, P., et al. (2021). No time dependence of ciprofloxacin pharmacokinetics in critically ill adults: comparison of individual and population analyses. Pharmaceutics, 13(8) 1156. **Q1, IF: 6.525**

15. Michaličková, D.*, Öztürk, H. K., Hroudova, J., et al. (2022). Edaravone attenuates disease severity of experimental auto-immune encephalomyelitis and increases gene expression of Nrf2 and HO-1. Physiol Res 71(1), 147. **Q3, IF: 2.1**

16. Michaličková, D*., Hartinger, J. M., Hladinová, Z., et al. (2022). Population pharmacokinetics-pharmacodynamics of fondaparinux in dialysis-dependent chronic kidney disease patients undergoing chronic renal replacement therapy. Eur J Clin Pharmacol 78(1), 89-98. **Note: shared first place of the authors Hartinger and Michalickova; Q3, IF: 2.9**

17. Pokorná, P., Michaličková, D.*, Völler, S., et al. (2022). Severity parameters for asphyxia or hypoxic-ischemic encephalopathy do not explain inter-individual variability in the pharmacokinetics of phenobarbital in newborns treated with therapeutic hypothermia. Minerva Pediatr 74(2), 107-115. **Q2, IF: 2.6**

18. Šantavý, P., Šíma, M., Zuščich, O., Kubíčková, V., Michaličková, D., et al. (2022). Population pharmacokinetics of prophylactic cefazolin in cardiac surgery with standard and minimally invasive extracorporeal circulation. Antibiotics 11(11), 1582. **Q1, IF: 4.8**

19. Michalickova, D.*, Kramarikova, I., Ozturk, H. K., et al. (2023). Detection of galanin receptors in the spinal cord in experimental autoimmune encephalomyelitis. Biomed Pap Med Fac Univ 167(1). **Q4, IF: 0.9**

20. Hartinger, J. M., Michaličková, D., Dvořáčková, E., et al. (2023). Intraperitoneally Administered Vancomycin in Patients with Peritoneal Dialysis-Associated Peritonitis: Population Pharmacokinetics and Dosing Implications. Pharmaceutics 15(5), 1394. **Note: shared first place of the authors Hartinger and Michalickova; Q1, IF: 5.4**

21. Urbánek, K., Šantavý, P., Zuščich, O., Kubíčková, V., Michaličková, D., et al. (2023). Population pharmacokinetic model-based dosing proposal for ampicillin prophylaxis in cardiac surgery patients with cardiopulmonary bypass. J Chemother 35(7), 614-622. **Q4, IF: 1.8**

22. Zavrelova, A., Sima, M., Malakova, J., Rozsivalova, P., Paterova, P., Zak, P., Visek, B., Michalickova, D., et al. (2023). Superiority of ceftazidime off-label high-dose regimen in PK/PD target attainment during treatment of extensively drug-resistant Pseudomonas aeruginosa infections in cancer patients. Br J Clin Pharmacol 89(4), 1452-1461. **Q2, IF: 3.4**

23. Pokorna, P., Michalickova, D.*, Tibboel, D., et al. Meropenem disposition in neonatal and pediatric extracorporeal membrane oxygenation. **Note: accepted for publication in *Antibiotics* (Q1, IF = 4.8)**

Abstract

Population pharmacokinetic (pop PK) modeling offers an advantage of identification of predictive covariates of a drug's PK variability. Identification of predictive covariates in a pop PK model represents a scientific base for creating personalized dosing regimens customized to individual patients. The aim of this habilitation thesis was to describe PK of drugs during specific therapeutic modalities in pediatric, neonatal, and adult population, to identify predictive covariates, and to propose optimal dosing of drugs during these specific therapeutic modalities.

This thesis represents a commented set of 7 original publications. The first part of the thesis discusses the PK of drugs in pediatric and neonatal population, whereas the second part deals with the PK of drugs in adult population.

In the first part, the influence of therapeutic modalities (extracorporeal membrane oxygenation, ECMO and therapeutic hypothermia) on the PK of phenobarbital and meropenem in pediatric and neonatal population was described. In accordance with the findings, current dosing regimens for these drugs were critically scrutinized and optimal dosing regimens were proposed.

In the second part of the thesis, the influence of therapeutic modalities (peritoneal dialysis, hemodialysis, extracorporeal circulation, ECC) on the PK of drugs in adults was described. We have described PK of vancomycin in end-stage renal disease (ESRD) receiving peritoneal dialysis. Additionally, simulations based on the model suggested that the existing dosing recommendations by the International society for peritoneal dialysis (ISPD) fail to achieve the desired drug exposure targets in the peritoneal cavity for the majority of patients with preserved diuresis and we have therefore proposed a new optimal dosing regimen. We have also described PK of fondaparinux in one ESDR patient undergoing peritoneal dialysis, in addition to those patients undergoing high-flux (HF) and low flux (LF) hemodialysis. Model-based simulations were performed, to illustrate the dosing implications of the final model of fondaparinux in ESRD patients. Finally, we have assessed the effect of conventional ECC on ampicillin PK in patients undergoing cardiac operation with cardiopulmonary bypass. Moreover, we have tested the impact of both conventional ECC and minimally invasive ECC on PK of cefazoline. Monte Carlo simulations have provided optimal dosing regimen for ampicillin and cefazolin in these patients.

Souhrn

Populační farmakokinetické (pop PK) modelování umožňuje identifikaci prediktivních kovariát a farmakokinetické (PK) variability léku. Identifikace prediktivních kovariát v pop PK modelu je vědeckým základem pro vytváření personalizovaných dávkovacích režimů přizpůsobených jednotlivým pacientům. Cílem této habilitační práce bylo popsat PK léků během specifických terapeutických modalit v pediatrické, novorozenecké a dospělé populaci, identifikovat prediktivní kovariáty a navrhnout optimální dávkování těchto léků.

Tato práce představuje komentovaný soubor 7 originalních publikací. První část této práce popisovala PK léků v pediatrické a novorozenecké populaci, druhá se zabývala PK léků v dospělé populaci.

V první části byl popsán vliv terapeutických modalit (mimotělní membránové oxygenace, angl. extracorporeal membrane oxygenation, zkráceně ECMO a terapeutické hypotermie) na PK fenobarbitalu a meropenemu v dětské a novorozenecké populaci. V souladu se zjištěními byly současné dávkovací režimy těchto léků kriticky přezkoumány a byly navrženy optimální dávkovací režimy.

V druhé části práce byl popsán vliv terapeutických modalit (peritoneální dialýza, hemodialýza a mimotělní oběh, angl. ectracorporeal circulation, zkráceně ECC) na PK léků u dospělých. Popsali jsme PK vankomycinu u pacientů v konečném stadiu renálního onemocnění (angl. end stage renal disease, zkráceně ESRD) na peritoneální dialýze. Simulace založené na modelu navíc naznačovaly, že aktuální doporučení mezinárodní společnosti pro peritoneální dialýzu (angl. International Society for Peritoneal Dialysis, zkráceně ISPD) ohledně dávkování nedosahují požadovaných cílů expozice léku v peritoneální dutině u většiny pacientů se zachovanou diurézou, a proto navrhly optimální režim dávkování. Popsali jsme také PK fondaparinuxu u jednoho pacienta s ESDR podstupujícího peritoneální dialýzu, navíc k pacientům podstupujícím vysokoprůtokovou (angl. high flux, zkráceně HF) a nízkoprůtokovou (angl. low flux, zkráceně LF) hemodialýzu. Konečně jsme odhalili, že konvenční ECC neměla žádný vliv na PK ampicilinu u pacientů podstupujících srdeční operaci s kardiopulmonálním bypassem. Na druhé straně naše analýza zjistila, že jak konvenční ECC, tak minimálně invazivní ECC snižují periferní Vd, zatímco plocha tělesného povrchu a odhadovaná rychlost glomerulární filtrace (angl. estimated glomerular filtration rate, zkráceně eGFR, jako marker funkčního renálního stavu) byly identifikovány jako významné kovariáty pro centrální Vd a CL, v daném pořadí. Simulace Monte Carlo poskytly u těchto pacientů optimální režim dávkování ampicilinu a cefazolinu.

Introduction

In clinical practice, achieving a successful outcome involves adhering to the five "rights" of drug administration: giving the right drug to the right patient at the right time, in the right dose, and through the right route. These principles are fundamental to the pharmacist's decision-making goals (1, 2). After selecting the appropriate drug for a specific condition, the key factor for a successful therapeutic outcome lies in determining the right dose. Dose individualization is crucial to ensure both the safety and efficacy of drug therapy, avoiding issues like toxicity from overdosing or therapeutic failure and resistance development in the case of antimicrobials from underdosing (3). Variations in patient demographics, pathophysiological conditions, and comedications can influence a drug's pharmacokinetics (PK), altering how much and how quickly the drug reaches its target site in the body. To address these variations in a quantifiable manner, covariates are incorporated into population pharmacokinetic (pop PK) models to optimize drug doses for individual patients. Predictive covariates are clinical or environmental characteristics which describe predictable sources of PK variability in a specific population. Identification of predictive covariates in a pop PK model represents a scientific basis for creating personalized dosing regimens customized to individual patients.

Pharmacometrics is a scientific discipline that involves mathematical and statistical modeling to understand, characterize, and predict the PK and pharmacodynamic (PD) properties of drugs, as well as biomarker-outcome behavior (2, 4). It combines principles from pharmacology, mathematics, statistics, and computer science to create quantitative models that describe the relationships between drug doses, concentrations in the body, and observed effects. Pharmacometrics plays a crucial role in meeting regulatory requirements for new drug development and informing clinical decision-making. It helps researchers and clinicians make informed decisions about drug efficacy, safety, and dosing strategies, particularly in populations with diverse characteristics. The use of pharmacometric models contributes to more efficient and rational drug development and improves the understanding of the relationships between drug exposure and response.

PK modeling

The model represents a simplified representation of the complex PK and PD processes, utilizing mathematical relationships to explain and predict how drugs behave in the body. PK modeling technique is a crucial tool in both clinical drug development and pharmacotherapy practice. Population modeling, a sophisticated process, requires meticulous procedures to ensure data cleanliness, suitable computing platforms, ample resources, and effective communication. This approach is not only economically efficient but also timesaving, providing a robust framework for integrating all information gathered during the evaluation of new drugs.

The developed model can be simulated, enabling the exploration of different study designs/dosing regimens (1). Simulation settings help assess the impact of various designs on study outcomes, such

as optimizing drug dosage regimens or regulatory affairs (obtaining drug approval). The PK modeling approach, integral part of pharmacometrics, is commonly implemented through pop PK and physiologically based pharmacokinetic (PBPK) modeling approaches. Schematic representation of these approaches is given in Figure 1.

PBPK and pop PK models possess significant descriptive and predictive capabilities, and this makes them valuable tools in decision-making processes across drug development and clinical pharmacotherapy (2). These approaches are not mutually exclusive but rather complementary in the field of PK. Pop PK models are traditionally considered empiric, as they incorporate theoretical features and characteristics grounded in data apprehension (5). Pop PK modeling is compartment-based, but these compartments usually do not have any distinct physiological meaning. Pop PK modeling builds a model that fits all the available PK information. Therefore, these models are called "top down," starting with observed PK data. Specific advantage of pop PK modelling is the ability to distinguish between interindividual variability (IIV) and intraindividual variability, or residual unexplained variability (RUV) and to quantify them. Understanding of IIV variability establishes the scientific foundation for creating rational and personalized dosing schemes tailored to individual patients (6). Pop PK method was used as the main method in this habilitation work and will be in detail explained in the next chapter.

PBPK models are "bottom up," starting with the information at the organ, or tissue level and are also compartment-based, but, contrary to pop PK, these compartments represent actual physiological entities (7). PBPK models consist of physiological entities, such as an organ or tissue, and the blood flow into and out of those entities. In PBPK models, compartments extend beyond entire organs; frequently, these models include nested compartments that depict various cell types within an organ and, at times, even different organelles within a cell. Due to their detailed construction, PBPK models are excellent at addressing specific questions. For instance, they can incorporate the molecular signature of a disease or specific physiological state, such as pregnancy, adjusting key parameters to predict changes in drug concentration within a particular patient population. Such predictions play a crucial role in guiding dosing recommendations and shaping the design of clinical trials, especially when evaluating a drug for a new indication. Predicting and simulating drug-drug interactions (DDI) is another application, contingent on knowing the metabolic and transport information for both drugs. However, PBPK models are limited by the available mechanistic knowledge; for example, predicting a DDI's impact is impossible without knowledge of the enzymes involved in drug metabolism. The capabilities of PBPK modeling can be extended by not only describing changes in drug concentration over time in specific compartments but also modeling the PD effects on tissues and organs (8). Despite these strengths, PBPK models can be limited by their complexity, making it challenging to estimate parameters using traditional statistical methods. Parameter adjustment based on *in vitro* or pre-clinical data is one approach, but this relies on data availability, which is often lacking during drug development. Additionally, uncertainties arise regarding whether parameters estimated from *in vitro* or nonclinical species align with human

parameters. Adjustments to variables can be made when human plasma concentration-time data are available, enhancing the model's fit.

Several software packages are used in the practice of pharmacometrics, such as NONMEM 7.4 by ICON, Phoenix WinNonlin NLME by CERTARA, Simcyp by CERTARA, and Monolix by Lixoft, and the open-source tools nlmixr2, PK-Sim and MoBi, developed by open systems pharmacology (2).

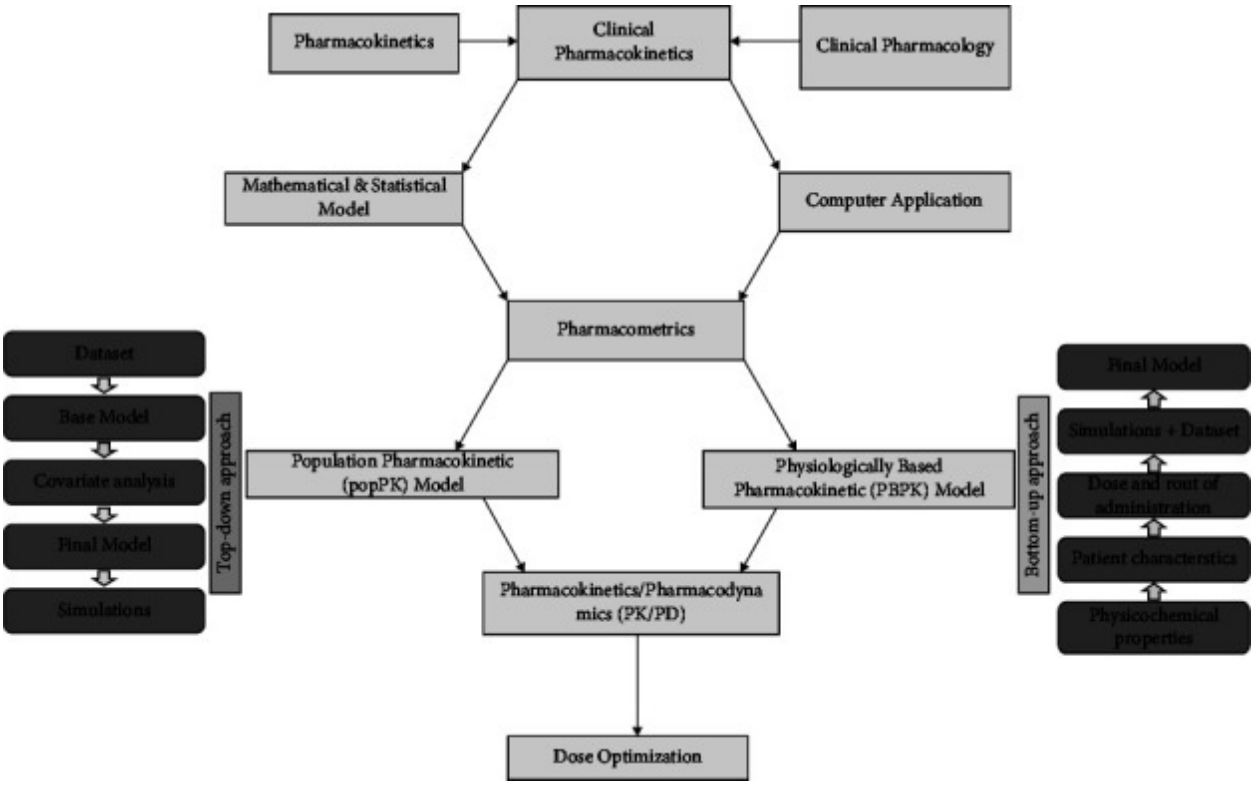

Figure 1. Main constituents of pharmacometrics (taken from (2))

Pop PK modelling

Approaches of pop PK modelling offer several advantages over traditional PK analysis (6). In the standard two-stage or classical approach, the process begins with estimating PK parameters individually based on each patient's concentration-time profiles (Figure 2). In the second step, the mean or median of these parameters is calculated, along with standard error or interquartile range (IQR) (these represent variability between subjects). However, a significant disadvantage of this methodology is its requirement for a relatively high number of samples in each individual; additionally, approximately the same number of samples must be provided by each individual. Furthermore, distinguishing between IIV and RUV is challenging. Consequently, there is a tendency to overestimate IIV (9). On the other hand, the pop PK approach conducts a simultaneous analysis of all data across the entire population, while still considering different observations originating from

different patients. Moreover, the population approach accommodates not only dense data but also sparse data (limited observations per individual) and unbalanced data (unequal distribution of observations throughout the concentration–time profile in individuals), or a combination of both. A specific advantage of this approach is its ability to differentiate IIV and RUV. As previously mentioned, this enables identification and quantification of predictive covariates, which represent the scientific base for creating personalized dosing regimens customized to individual patients.

Pop PK analysis uses non-linear mixed effects (NMLE) modeling approach. The term "mixed" denotes a combination of fixed and random effects. Fixed effects do not vary between the patients and represent a specific value of PK parameters, such as clearance (CL) and volume of distribution (Vd), for a one-compartment model (10, 11). Random effects account for the unexplained variability and consist of both intra-subject variability and IIV, as illustrated in Figure 2. These random effects are estimated simultaneously and separately. A common assumption is that the variability between subjects follows a normal distribution with a mean of zero and variance ω^2. Equation 1 is employed to depict the relationship between individual and population parameter estimates.

$\theta_i = \theta_{mean} * e^{\eta i}$ (1)

where θ_i, θ_{mean} and ηi denote the parameter of the i^{th} subject, the population mean, and the variability between subjects, respectively.

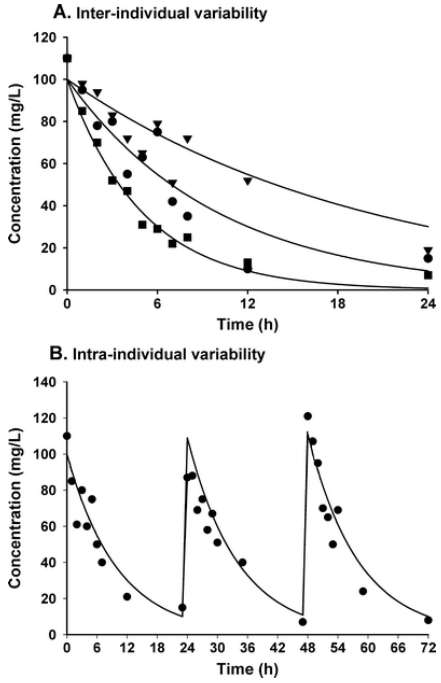

Figure 2. Levels of unexplained variability: A. inter-individual variability B. intra-individual variability (taken from (6))

The residual error describes intra-individual variability (more commonly denoted as RUV). RUV encompasses all those deviations in concentration which are not derived from IIV. It originates from

assay error, errors in recording sampling times, errors in dosage preparation and administration, and model misspecification. The residual error can be described using a proportional error (Eq. 2) or an additive error (Eq. 3) or a combination of both. Therefore, for the jth observed concentration of the Ith individual the relation (Y_{ij}):

$Y_{ij} = C_{predi,j} * (1+ \varepsilon_{i,j})$ (2)

$Y_{ij} = C_{predi,j} + \varepsilon_{i,j}$ (3),

where C_{pred} is predicted concentration and ε_{ij} is a random variable with a mean of zero and a variance of σ^2.

Pop PK model development

Generally, building a pop PK model requires 3 steps (6, 10, 11). The first step is the development of a structural model, where fixed effects are estimated. Subsequently a statistical model, estimating random effects, is designed and finally a covariate model is identified. These three models are mutually interrelated: for instance, the choice of structural model will influence choice of covariate model and vice versa. The task of identifying a model that accurately depicts the data involves a comprehensive process, where multiple steps of model inspection and refinement are undertaken. To evaluate the model's fit concerning observed concentrations or effect measures, scatter plots or goodness-of-fit (GOF) plots (described in the section *Validation of the PK–PD models*) are generated and objective function values (OFV) are calculated.

The structural model characterizes the standard concentration-time pattern observed within the population. The structural model (one-, two-, or three-compartment) is usually selected based on *a priori* information of drug disposition (12). When selecting the number of compartments for a model, it's important to consider that models with too few compartments result in poor data description, indicated by higher OFV and biased plots of residuals vs. time (11). Conversely, models with an excessive number of compartments exhibit only marginal improvements in OFV when adding extra compartments. Moreover, parameters for additional peripheral compartments may include values with minimal impact on plasma concentrations, such as (physiologically implausible) high Vd and low intercompartmental CL, or vice versa. In addition, parameters may be estimated with poor precision. Estimated parameters in the structural model are called “typical values”.

Statistical model depicts variability around the structural model. As previously mentioned, there are two levels of variability on NMLE modelling: IIV and RUV. Development of a proper statistical model is especially important for subsequent development of a covariate model, as inclusion of a statistically significant covariate into the model decreases IIV (11).

Covariate model development consists of identification of predictive covariates, which can be demographic characteristic (age, body weight (BW), sex), physiological/pathophysiological characteristic (hepatic or renal function), environmental characteristic or use of comedication or other treatment modality, such as extracorporeal membrane oxygenation (ECMO), hemodialysis,

peritoneal dialysis. As previously explained, identification of predictive covariates for variability represents the scientific base for rational and individualized dosing regimens.

During a systematic process of predictive covariates identification, scatter plots and summary plots are employed to assess individual parameter estimates and/or conditional weighted residuals (CWRES) relative to covariates. These plots help identify potential covariates, and investigate their nature (linear, exponential, allometric, subpopulations, etc.), and guide the forward inclusion of likely candidates into the model. Each covariate's influence is individually examined and compared with the base model (no covariates) to determine statistical improvement, typically assessed by the difference in OFV or log–likelihood ratio. A reduction in objective function of 3.84 is considered to be significant ($p < 0.05$) (13, 14). Additional criteria for covariate inclusion are visual improvement in GOF of the base model, the confidence interval (CI) of the parameter estimates, and the correlation matrix. Importantly, IIV and/or RUV is expected to be reduced. Finally, the obtained parameter values in the final covariate model should be physiologically plausible. This extensive procedure of covariate modelling indicates that each covariate is only included in the model if it can be entirely warranted by the data and the results of the statistical calculations.

When several covariates are found to be statistically significant, the covariate with the highest reduction in OFV compared to the base model is included and the other covariates are again tested for their significance. Following the incorporation of all covariates that significantly reduced the OFV in the base model, a backward deletion is initiated. This involves systematically removing each covariate from the full model, one at a time, starting with the one causing the smallest increase in the objective function. Statistical testing (OFV increase) is conducted to assess whether retaining or removing each covariate is justified. This process continues until each covariate has been subjected to the statistical evaluation for retention or removal.

Pop PK model validation

A famous British statistician George Box once wrote: “Remember that all models are wrong; the practical question is how wrong do they have to be to not be useful” (15). Therefore, to decide whether a model is useful and valid for clinical simulations, a meticulous evaluation and validation of the model is required. A final pop PK model can be validated externally, or internally. External validation implies the ability of the model to describe one or more external datasets adequately. External validation stands as the most compelling evidence supporting the validity of a pop PK model (16). However, the number of patients in the dataset is often limited, so internal validation methods are often employed, because they do not require additional datasets. Internal model validation consists of several procedures. The most often used are basic GOF plots, bootstrap analysis, Jackknife method, visual predictive check (VPC) and normalized prediction distribution error (NPDE). GOF plots are used for both external or internal validation, to discover any trends or bias of the final model (6). As previously mentioned, they are also one of the basic tools for model building. GOF plots consist of 4 plots:

1. Individual predicted vs observed concentrations
2. Population predicted vs observed concentrations
3. CWRES vs time (or time after last dose)
4. CWRES vs population predicted concentrations

CWRES are calculated according to the equation (4):

$CWRES = \frac{\vec{y}_i - E_{FOCE}(\vec{y}_i)}{\sqrt{Cov_{FOCE}(\vec{y}_i)}}$ (4)

where $\vec{y}_i$, $E(\vec{y}_i)$ and $CovFOCE(\vec{y}_i)$ are the vector of the measurements, the expectation of the data and the covariance matrix of the data, respectively (17).

In the **bootstrap method**, multiple replicate datasets are created by randomly selecting individuals from the original dataset (18). Each individual can be drawn multiple times or not drawn at all for each replicate. To accurately represent parameter distributions, a substantial number of replicates (e.g., ≥1000) are generated and assessed using the final model. The resulting parameter estimates from these replicates are compiled, and percentile bootstrap CIs are established by extracting the lower 2.5% and upper 97.5% values of each parameter estimate from the runs, regardless of convergence status (except for abnormal terminations). This interval encompasses the true value of the parameter estimate approximately 95% of the time, without assuming symmetry in the distribution.

Jackknife method is utilized to identify outliers in the dataset and individuals having a high impact on covariate selection (18). Usually, it is used when datasets with small number of individuals are analyzed. In the Jackknife method, each patient at a time is excluded from the dataset and all model parameters in the final model are re-estimated. Subsequently, population estimates from the jackknife samples are compared with the estimates of the final model. In this way, individuals that have a large influence on the parameter estimates are identified.

In a **VPC**, multiple (usually 1000) simulations of PK or PD profiles are performed (6). The resulting graph includes lines representing the median values and their 90% prediction intervals. Observations from the internal or external dataset are overlaid on this graph. The visual inspection involves checking if 90% of the observed values fall within the indicated prediction interval and assessing for any bias compared to the interval. This method doesn't involve statistical tests; instead, assessments are made through visual inspection. Its interpretation is usually easy when the individuals in the analyzed dataset are similar. However, when a significant deviation between individual profiles is expected, for instance due to substantial variability in dose timing or amount of administered drug, or when numerous covariates are present, the application of this diagnostic tool becomes more challenging (6).

NPDE is another simulation-based tool, which is appropriate for both external and internal validation of the final model (6). Unlike the VPC, NPDE provides information on how accurately the model predicts both the median value of observations and the variability within them. While the interpretation of NPDE is less straightforward than VPC, it offers an advantage in scenarios with high

variability in dosing regimens or when a large number of covariates are present in the model. This is particularly useful for data obtained during routine clinical practice. Software tools, such as the NPDE add-on package for R (19), are freely available for conducting this analysis. In addition to visual evaluation, NPDE allows for statistical tests, and these tests are known to be highly sensitive and powerful. Therefore, decisions regarding the model should primarily rely on visual assessments, considering potential statistical significance with caution.

Pop PK in pediatric population

Children exhibit distinct responses to drugs compared to adults, influenced by variations in both PK and PD. These differences may further vary across different age groups of children. Throughout a child's growth, there are developmental changes in enzyme pathways (related to PK) and the function and expression of receptors and proteins (related to PD). These changes, often termed "developmental changes" in childhood, occur at varying rates across different pathways and receptors. Importantly, these rates do not always align solely with the increase in the child's BW. Therefore, the challenge lies in acquiring data in children that enable the exploration of these developmental changes, ultimately leading to the establishment of evidence-based dosing regimens for drugs in the pediatric population (6).

Developmental changes in childhood can impact all PK processes, ranging from drug absorption to elimination, but also PD effects. For instance, neonates exhibit an elevated intra-gastric pH (>4), potentially affecting the bioavailability of acid-labile compounds like penicillin G and weak acids such as phenobarbital when administered orally (20). Additionally, neonates experience delayed gastric emptying, leading to slower drug absorption, for example, in the case of paracetamol (21). Moreover, children undergo changes in metabolizing enzyme capacity. While most uridine 5'-diphosphate-glucuronosyltransferases (UGTs) and P-450 cytochromes are expressed within the first week of life, their activity at birth is typically low compared to adults. For example, UGT2B7 activity at birth is approximately 10% of the adult level. Moreover, various enzyme systems are recognized to mature at different rates during early development (20, 22, 23).

Physiological changes with age impact renal function and liver flow. The glomerular filtration rate (GFR) in full-term neonates, measured in mL/min/70 kg, is 35% of the adult value, reaching adult values at approximately 1 year old (24). However, it's essential to recognize that even when corrected for body weight differences, actual GFR values in children remain substantially lower than those in adults.

Moreover, the continuous changes in body composition in children result in an age-dependent proportion of body water and fat, influencing drug distribution (25). For instance, neonates have a higher total amount of body water (80–90% of body weight) compared to adults (55–60%), impacting the Vd for hydrophilic drugs like aminoglycosides. This can be attributed to the larger amount of extracellular fluid (45% of body weight) in neonates compared to adults (20%).

To understand how developmental changes in childhood affect the PK of a drug, it is essential to obtain concentration–time profiles, which necessitate measurements of drug concentrations. In pediatric studies, ethical considerations mandate limitations on discomfort, such as pain and anxiety related to venipuncture (6). Practical constraints also restrict the volume and quantity of blood samples that can be collected. Due to the typically limited number of samples feasible in pediatric subjects, the preferred approach for obtaining PK and PD parameters is the population approach using NMLE. When planning a pediatric study with data analyzed using the population approach, it is recommended to collect samples at various times or use alternating sampling schemes in patient subgroups. This approach allows for the collection of samples during routine clinical sampling, reducing the burden on participating children. This strategy ensures that the statistical power to develop a model describing the concentration–time or concentration–effect profile is not compromised or enhanced.

The aim of this habilitation thesis was to describe PK of various drugs during specific therapeutic modalities, in neonatal, pediatric and adult population, to identify predictive covariates, and to propose optimal dosing of these drugs during these therapeutic modalities.

Methods

Demographic data

Study 1 (appendix 1) was a retrospective study which aimed to assess the effect of ECMO on phenobarbital PK in neonates. Data from 13 critically ill neonates with a median birth BW of 3.21 kg (IQR: 2.65–3.72) kg, postnatal age (PNA) at start of treatment: 2 (0–7) days and gestational age of 38 (38–41) weeks receiving veno-venous (VV) or veno-arterial (VA) ECMO were analyzed. Blood samples were collected during therapeutic drug monitoring (TDM). In total, there were 55 phenobarbital concentrations, including 5 concentrations before ECMO, 31 during ECMO, and 19 concentrations after ECMO. Phenobarbital was dispensed intravenously (i.v.) with a loading dose (LD) of 7.5 (8.5–16) mg/kg administered in 15 minutes. Additional LD was given if clinically indicated until a maximum total LD of 40 mg/kg was achieved. I.v. maintenance dose (MD) of 6.9 (4.5–8.5) mg/kg/day was given in 2 doses every 12 hours administered in 15 minutes (11). Adjustments in dosing were made based on clinical and/or amplitude-integrated electroencephalography response.

Study 2 (appendix 2) aimed to assess the impact of therapeutic hypothermia, as well as parameters for asphyxia and hypoxic-ischemic encephalopathy (HIE) on PK of phenobarbital in newborns. 120 plasma samples from TDM were collected from 50 neonates, with a median BW of 3.3 (2.8-3.5) kg and gestational age of 39 (39-40) weeks. Phenobarbital was administered in the same way as described for study 1. Phenobarbital treatment started at 0.5-6.0 h after asphyxia insult during the therapeutic window to induce therapeutic hypothermia.

Study 3 (appendix 3) aimed to assess PK of meropenem in neonatal and pediatric patients undergoing ECMO. It involved 45 critically ill patients (38 received ECMO) with a median BW of 7.88 (3.62 – 11.97) kg and PNA of 3 (0 – 465) days. A total of 152 meropenem plasma concentrations were available for analysis, including 94 concentrations collected during ECMO. Blood samples were collected during TDM. Meropenem was administered to infants younger than 3 months of PNA over a 30-minute short infusion (SI) and over 15-30 minutes of SI in older children, i.v. in a dose of 20 to 40 mg/kg 2-4 times a day.

Study 4 (appendix 4) aimed to evaluate PK of vancomycin in patients undergoing peritoneal dialysis. Data were obtained from 41 patients with end-stage renal disease (ESDR) with BW of 75 (70–84) kg and age of 68 (53–74) years during 57 hospitalization occasions; analysis included 132 or 241 peritoneal and plasma vancomycin concentrations, respectively. During these instances, patients received treatment for suspected or culture-validated peritonitis, encompassing recurrent and relapsing episodes. The individual regimen included 4–5 manual exchanges per day (continuous ambulatory peritoneal dialysis, CAPD). In majority of the patients, International Society for Peritoneal Dialysis (ISPD) recommendations were followed, consisting of a LD of 15–30 mg/kg followed by MD of 25 mg/L of peritoneal dialysate in all subsequent exchanges (26). The plasma concentrations were monitored and MD was adjusted to achieve the target AUC_{24} for vancomycin

plasma concentrations of 400–600 mg×h/L, recommended by Rybak et al (27). In a case of systemic infection, i.v. dosing was combined with i.p. dosing. Three patients who received only i.v. dosing were also added to the database; i.p. levels from these patients were available.

Study 5 (appendix 5) was a retrospective study which described PK of anti-Xa activity (112 samples) from 12 (3 male and 9 female) ESRD patients with age of 71 (63–88) years and BW of 73 (59–98.5) kg. 11 patients received high-flux (HF) or low-flux (LF) hemodialysis and one patient underwent peritoneal dialysis. Additionally, 3 patients also underwent therapeutic plasma exchange (TPE). Typically, fondaparinux was administered 3 times weekly before the hemodialysis session. Additional doses, not accompanied by dialysis, were given when necessary, such as extra doses at the beginning of therapy to achieve effective anticoagulation promptly. Patients receiving fewer than three dialysis sessions per week received additional doses for palliative reasons or due to residual renal function, aiming to reduce hospital visits. Generally, an LD of 2.5 mg of fondaparinux was administered during the first hemodialysis session. If an insufficient anti-Xa level was measured after hemodialysis, an additional dose (2.5 mg) was added. This dosing procedure was repeated in the following sessions. For long-term treatment in ESRD patients, a MD of 2.5 (1.5–2.5) mg was given every hemodialysis session. The patient undergoing peritoneal dialysis received an LD of 2.5 mg and an MD of 0.5 mg/day. Fondaparinux was administered either i.v. at the beginning of the HD session (92% of the occasions) or subcutaneously (s.c.) if a dose was administered at a different time (8% of the occasions). Blood samples were collected during TDM. The analysis included 112 anti-Xa levels.

Study 6 (appendix 6) aimed to assess the effects of standard extracorporeal circulation (ECC) on PK of ampicillin used prophylactically in cardiac surgery. It was a prospective study which included 40 patients (20 patients receiving ECC and 20 control patients). In total, 273 blood samples were collected. 2000 mg of ampicillin (in combination with 1000 mg of sulbactam) was administered 30–60 min before the surgery onset. Blood samples were collected at 15, 30, 45, 60, 120, 180 min after the ampicillin administration and at the end of the surgery.

Study 7 (appendix 7) aimed to assess the effects of both existing types of cardiopulmonary bypass: standard ECC and minimally invasive ECC (MiECC) on PK of cefazolin in patients undergoing cardiac surgery. It was a prospective study which involved 65 patients, including 25 (19 male, 6 female) patients receiving MiECC support, 20 (19 male, 1 female) patients receiving ECC support, and 20 (17 male, 3 female) patients with no ECC/MiECC treatment. In total, 461 collected samples were obtained for the PK analysis. An i.v. bolus of 2000 mg of cefazolin was administered 60–30 min before the onset of the cardiac surgery. Samples were collected at 15, 30, 45, 60, 120 and 180 min after cefazolin administration and at the end of the surgery.

The data analysis of data was executed using NONMEM Version 7.3.0 (ICON Development Solutions, Ellicott City, MD) and PsN v3.4.2 (28, 29) both running under Pirana 2.9.0 (30) or using Monolix (Lixoft, Paris, France). For the visualization of the data and model diagnostics for the models

developed by NONMEM, R (different versions for different models, for more details, please see each individual research paper (appendices 1-7) was used.

Model development

Model development was carried out in three steps.

1. **Development of structural and statistical model:**

For the structural model, to describe the distribution of investigated drugs, one- and two-compartment models were tested. First-order CL of drugs was assumed. Log-normally distributed IIV terms with estimated variance were analyzed on each PK parameter. For the residual error model, proportional, additive, and combination error models were tested.

In **study 5,** fondaparinux was administrated s.c. in 8% of cases and as samples were not collected shortly after administration, the estimation of the absorption rate of fondaparinux was not feasible. Consequently, it was assumed that the absorption occurred instantaneously. The bioavailability of the subcutaneous doses was also assumed to be 100%, consistent with previous publications (31). In this study, pop PK-PD analysis was conducted. Structural PK model was developed as previously described; for the PD aspect, the relationship between anti-Xa activity and fondaparinux concentration was fixed at 1.18 IU/µg, determined by the laboratory-specific value from our laboratory. Various statistical distributions, including normal and log-normal distributions, were tested for the IIV terms on this slope parameter.

2. **Development of a covariate model:**

Different covariates, in accordance with the specific aim of the study, were tested. For more details of the tested covariates, please see each individual research paper (appendices 1-7).

A stepwise covariate modeling procedure was executed. Multiple time-varying measurements were used for all continuous covariates. Continuous covariates were tested in linear and power functions, whereas categorical covariates were tested by estimating the parameter value for one category as a fraction of the parameter value for the other category.

For model selection, reduction in OFV of more than 3.84 points between nested models ($p < 0.05$) was regarded as statistically significant, assuming a chi-square test distribution. Further criteria for model selection were relative standard error (RSE) of the estimates of structural model parameters less than 50%, physiologic plausibility of the parameter estimates, and absence of bias in GOF plots.

In study 1, during prolonged ECMO treatment in neonatal population, it was difficult to distinguish impact of maturation, clinical improvement/disease progression, and influence of ECMO from each other. Therefore, maturation functions for CL and Vd were obtained from literature and were included in the model (32). Firstly, it was verified that phenobarbital concentrations off ECMO can be accurately described by the previously published model. Subsequently, the following covariates were tested: disease status (laboratory values of serum creatinine, urea, albumin, direct and total

bilirubin, C-reactive protein (CRP), blood pH, aspartate transaminase, and alanine transaminase, urine output) were tested as continuous covariates; concomitant treatment modalities (use of diuretics, inotropes, therapeutic hypothermia and continuous renal replacement therapy, CRRT) were tested as categorical covariates; ECMO parameters: on/off ECMO, ECMO circuit change, and ECMO modalities (VV, VA), were tested as categorical covariates and speed, flow, duration, time after onset and decannulation of ECMO were tested as continuous covariates.

Study 2 tested the following continuous covariates: PNA, gestational age, and BW, and the following categorical covariates: pH of arterial umbilical cord blood categorized as ≥7 or <7, Apgar score at the 1^{st}, 5^{th} and 10^{th} minute, categorized as ≤5 or >5, base excess (BE) in arterial umbilical cord blood categorized as deficit ≥12 mmol/L or <12 mmol/L, serum creatinine level categorized as ≤140 µmol/L or >140 µmol/L, serum lactate level categorized as ≤3 mmol/L or >3 mmol/L, comedication with other anti-epileptic drugs, presence of HIE defined according to the latest guidelines (33), as Apgar at 5^{th} and 10^{th} minute <5 and pH of arterial umbilical cord blood <7 or base deficit in arterial umbilical cord blood deficit ≥12 mmol/L or both and appropriateness for cooling defined as pH of arterial umbilical cord blood ≤7 or base deficit in arterial umbilical cord blood deficit ≥16 mmol/L and Apgar score at 10^{th} minute <5 (34). For the purpose of data analysis, severe asphyxia was defined as pH of arterial umbilical cord blood ≤7.1 and Apgar score at the 5^{th} minute ≤5, and severe HIE was defined as time to normalization of aEEG >24 h, similarly as in the previous analysis (35).

Study 3 tested the following covariates: maturation status (BW and PNA), disease status (laboratory values of serum creatinine, urea, albumin (at the start of the treatment and also during whole course of treatment), total bilirubin, CRP, blood pH, aspartate transaminase, and alanine transaminase, pediatric index of mortality (PIM) score) were tested as continuous covariates; concomitant treatment modalities (use of diuretics, inotropes, and CRRT) were tested as categorical covariates; ECMO parameters: on/off ECMO, ECMO circuit change, and ECMO modalities (VV, VA), were tested as categorical covariates and speed, flow, duration, time after onset and decannulation of ECMO were tested as continuous covariates.

Study 4 tested the following continuous covariates: BW, lean body mass, age, serum level of urea, albumin, creatinine, potassium, CRP at the beginning of the peritonitis treatment, eGFR (calculated by the CKD-EPI 2009 formula), and volume of residual diuresis. Sex, preserved diuresis (yes = over 500 mL daily urine output or no = less than 500 mL daily urine output), and peritoneal solution type (low, medium, or high glucose content, or icodextrin based) were tested as categorical covariates.

Study 5 tested the following continuous covariates: BW, age, and length of hemodialysis. Tested categorical covariates were sex, presence of residual diuresis, type of hemodialysis (i.e., high flux (HF)/low flux (LF)/no hemodialysis), use of TPE (i.e. on/off TPE), presence of oliguria.

Study 6 tested continuous covariates: BW, height, body surface area (BSA), age, serum level of creatinine, total protein, total bilirubin, albumin, urea and eGFR calculated according to the CKD-EPI formula. Sex and ECC/MiECC modality were tested as categorical covariates.

Study 7 tested BW, height, BSA, age, body temperature, preoperative serum levels of total bilirubin, albumin, total protein, urea and creatinine, and eGFR as continuous covariates, whereas sex and the use of ECC were tested as categorical covariates.

3. Validation of the model

For internal validation of the final models, bootstrap method (Jackknife method for studies 1 and 5), NPDE or VPC were used. The predictive properties of the structural and statistical models were checked by NPDE and VPC. For NPDE, the original dataset was simulated 500 (or 1000) times, after which the observed concentrations were compared with the range of simulated values using the NPDE package developed for R (19). For VPC, 1000 replicates of the original dataset were simulated using the parameter estimates of the final model, and the distributions of the observed and simulated data were then compared. The 90% prediction intervals for the 10th, 50th and 90th percentiles of the simulations were calculated from all replicates and presented graphically. To test the stability of the model, a bootstrap analysis was carried out. For this, 500 (or 1000) replicates of the original data were created, and the parameter estimates for each sample were re-estimated. The median and 95% CI acquired for each of the parameters estimated from the bootstrap samples were then compared with the final model parameter estimates. For jackknife method, each subject a time was excluded from the dataset and all model parameters in the final model are re-estimated. Population estimates from the jackknife samples were then compared with the estimates of the final model.

Simulations for dosing implications

To illustrate the dosing implications of the final pop PK models (studies 1, 4, 5) simulations were executed with the final population pharmacokinetic model, which included IIV in model parameters, to explore the probability of target attainment.

For neonates undergoing ECMO (study 1), 1000 simulations for neonates with a birth BW (bBW) of 3.21 kg and PNA of: 0, 7, 14, 21 days were carried out for a LD of 20mg/kg and different maintenance doses (MD). For MD, simulations consisted of a dose of 5 mg/kg/d for newborns of PNA of 0–14 days and a dose of 6 mg/kg/d for newborns of PNA of 15–28 days divided in 2 daily doses (these are the recommendations of the Dutch National Children's Formulary (36)). Simultaneous onset of ECMO and phenobarbital treatment was assumed. Simulations were performed for 12 days, as this duration was supported by the model (the longest individual duration of ECMO was 12 days). No target concentrations have yet been defined for newborns receiving phenobarbital for neuroprotection and sedation, target concentrations for newborn seizures (15–40mg/L) were utilized (36).

For patients undergoing peritoneal dialysis (study 4), 1000 simulations for a typical individual with BW of 75 kg and estimated glomerular filtration (eGFR) of 6.76 mL/min with preserved diuresis and oliguria were executed for dosing regimens recommended by the International Society for

Peritoneal Dialysis (25 mg/kg once every 5 and 7 days - intermittent dosing, and a LD of 25 mg/kg followed by MD of 25 mg/L in each subsequent exchange - continuous dosing) over 21 days. Only continuous dosing was simulated for patients with eGFR = 6.76 mL/min, 50 kg and 100 kg with oliguria and preserved diuresis, because this dosing regimen is typically followed in our medical center. Subsequently, simulations with the newly proposed dosing regimen were performed. This new dosing regimen can improve intraperitoneal vancomycin exposure without achieving toxic plasmatic levels.

For patients on HF and LF hemodialysis (study 5), 1000 simulations were executed for LD of 2.5 mg and 5 mg both in combination with a MD of 2.5 mg administered 3 times weekly for 4 weeks.

Simulations for dosing optimization

Monte Carlo simulations based on final pop PK models of antibiotics (studies 3, 6 and 7) were performed to predict probability of target attainment (PTA) using Simulx version 2021 (Lixoft SAS, Antony, France).

For pediatric patients undergoing CRRT (study 3), 10000 Monte Carlo simulations were executed for infusion lasting 0.5 and 3 h for doses of 20mg/kg and 40 mg/kg of meropenem every 8 h and continuous infusion of 60 and 120 mg/kg/day for individuals with BW of 7.88 kg (typical individual), as well as 3.92 kg (25^{th} percentile of BW range) and 11.97 kg (75^{th} percentile of BW range), on and off continuous renal replacement therapy for 7 days. Then, %T > MIC was calculated for each individual and a PTA was obtained by counting the percentage of individuals who achieved 40% or 100% T > MIC for MIC values ranging from 0.5 to 16 mg/L.

For patients undergoing cardiac surgery with ECC (study 6), standard prophylactic ampicillin dosing regimen of 2000 mg i.v. was simulated for various degrees of renal impairment: (<1, 1–1.5, 1.5-2.17 and >2.17mL/s/1.73m^2). PK/PD targets were defined as 50% and 100% of time when the plasmatic concentrations of unbound ampicillin are above the MIC throughout the dosing interval (50% T>MIC and 100% T > MIC). The MIC values of 2 mg/L (non-species related breakpoint according to EUCAST) and 8 mg/L (breakpoint for Enterobacterales according to EUCAST) were used for simulations. As PK/PD targets involve the unbound fraction of ampicillin concentrations, a correction factor of 28% for the binding of ampicillin to plasma proteins was accounted for the in the simulations. The dosing regimen was considered to be successful if ≥95% of patients achieved the PK/PD target.

For patients undergoing cardiac surgery with standard ECC and MiECC (study 7), 500 Monte Carlo simulations based on the final cefazolin model were performed. Simulations included 2000 mg i.v. (standard dosing regimen) for patients with various renal statuses (eGFR < 1 mL/s, 1–2.17 mL/s and >2.17 mL/s). PK/PD target was defined as the 100% of time above the MIC throughout the dosing interval (100% T > MIC). The PTA was calculated for various MIC values (0.25, 0.5, 1, 1.5. 2, 3 and 4 mg/L). The dosing regimen was considered to be successful if ≥90% of patients achieved the PK/PD target.

Results

All results are extensively presented in the publications. Only the main results are presented here.

Pop PK studies in pediatric population

Study 1: during prolonged ECMO treatment in neonatal population, it is difficult to distinguish impact of maturation, clinical improvement/disease progression, and influence of ECMO from each other. Therefore, maturation functions for CL and Vd were obtained from literature and were included in the model (32). Firstly, it was verified that incorporating maturation functions into the model resulted in accurate predictions of phenobarbital concentrations both before the initiation of ECMO and after ECMO discontinuation. This implied that patients off ECMO and those from the previously published model were similar in terms of the maturational status of phenobarbital PK.
Afterwards, other covariates (for liver function, renal status, ECMO properties, etc.) were tested in the model. One-compartment model was found to provide the best description of distribution of phenobarbital. For a typical neonate off ECMO with a median birth BW of 3.21 kg at a median PNA of 2 days, the CL and Vd were 0.0096 L/hr (RSE = 11%) and 2.72 L (16%), respectively (Table 1). Phenobarbital CL linearly increased with time during ECMO treatment, whereas after decannulation, CL primarily reduced and later gradually increased due to maturation. No changes in Vd associated with ECMO treatment were observed, possibly due to sparse sample collection shortly after onset of ECMO.
Despite the limited number of patients and samples, the diagnostics and validation of the model suggested that the developed model was accurate and robust. GOF plots (Figure 3) showed there was no bias in description of individual and population predicted concentrations of phenobarbital before, during or after cessation of ECMO. Additionally, accuracy of the model was also confirmed by NPDE distribution (Figure 4), where mean was -0.0799 and variance was 1.034. Neither mean nor variance significantly deviated from the expected values of 0 ($p = 0.53$) and 1 ($p = 0.56$), respectively. Finally, Jackknife analysis confirmed that no individual significantly influenced the estimated parameters values.

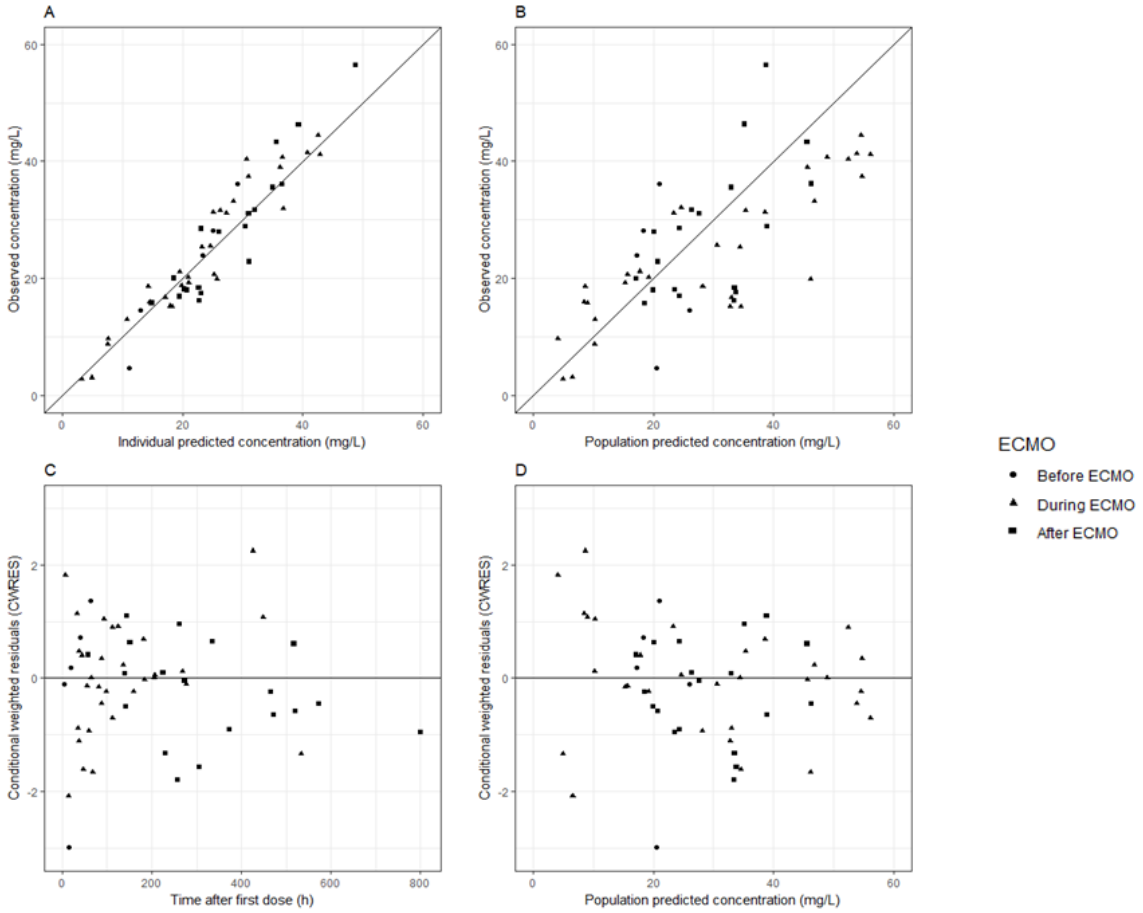

Figure 3. Goodness of fits plots for the final model of phenobarbital pharmacokinetics in neonates on extracorporeal membrane oxygenation. A. Population predicted phenobarbital concentration vs. observed phenobarbital concentration. B. Individual predicted phenobarbital concentration vs. observed phenobarbital concentration. C. conditional weighted residuals (CWRES) vs. time after dose. D. Conditional weighted residuals (CWRES) vs. population predicted concentration.

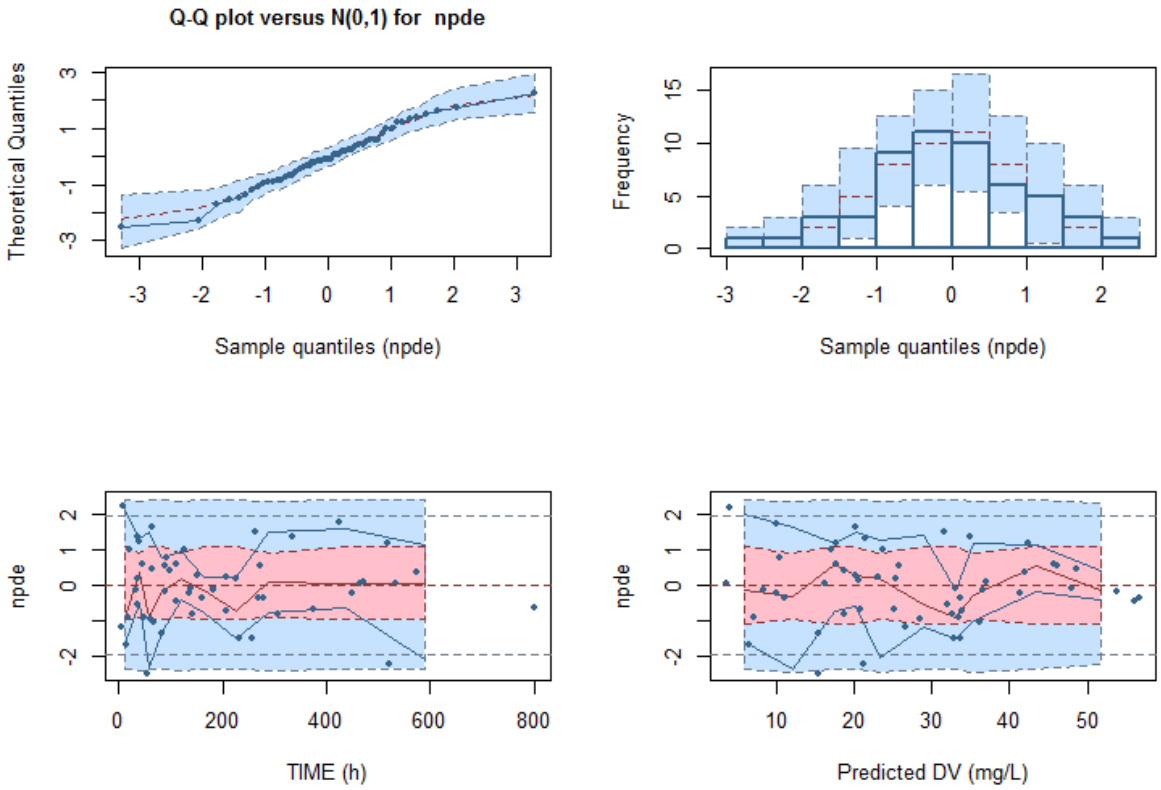

Figure 4. Visual output of the normalized prediction distribution error (NPDE) analysis. Shown at the top are the QQ plot and histogram of the NPDEs in the overall dataset. The red dotted line and blue shaded areas show the expected trends and 95% confidence intervals of these trends, while the dark blue lines and bars show the observed NPDE distributions. At the bottom, the individual NPDE values for each observation are plotted versus time and versus the predicted concentrations with the symbols. The solid lines in the bottom graphs indicate the mean (red) and the 90% percentiles (blue) of the NPDEs, and the shaded areas are the simulated 90% confidence intervals of the NPDE median (red) and 90% percentiles (blue), while the dotted red and blue lines show the expected values for the median and 90% percentiles. Numerical prediction distribution errors (NPDE) of the final model: mean = -0.0799 and variance = 1.034.

Table 1. Population PK model parameters of phenobarbital in neonates undergoing ECMO

Parameter [unit]	Final model (RSE %)
Fixed effects	
CL [L/h] = CLp * (1 + θbBWCL*(bBW - 2.59)) * (1 + θPNA*(PNA - 4.50)) * (1 + θTECMO * (TECMO/109))$^{ECMO\_on}$	
CLp [L/h]	0.0096 (11%)
θbBWCL	0.369 FIX
θPNA	0.0533 FIX
θTECMO	1.09 (28%)
Vd [L] = Vp * (1 + θaBWV * (aBW - 2.70))	
Vp [L]	2.72 (16%)
θaBWV	0.309 FIX
Inter-individual variability	
CL (%)	29.4 % (26%)
Vd (%)	45.3 % (17%)
Residual unexplained variability	
Proportional (%)	4.41 (32%)

Abbreviations: RSE = relative standard error of the estimate; CL = clearance; CL = population clearance value; θbBWCL = increase in CL per kg birthweight; θPNA = increase in CL per postnatal day (PNA); ΘTECMO = increase in CL per h time after ECMO cannulation (TE); ECMO_on = binary parameter designating ECMO treatment is on (1) or off (0); Vd = volume of distribution; V = population volume of distribution value; θaBWV = increase in Vd per kg actual body weight; bBW = birth body weight; aBW = actual body weight

The model implied that target attainment is achieved within the first 12 days of ECMO with a regimen consisting of an LD of 20 mg/kg and an MD of 4 mg/kg/day divided into two doses, with an increase of 0.25 mg/kg every 12 hours during ECMO therapy (Figure 5).

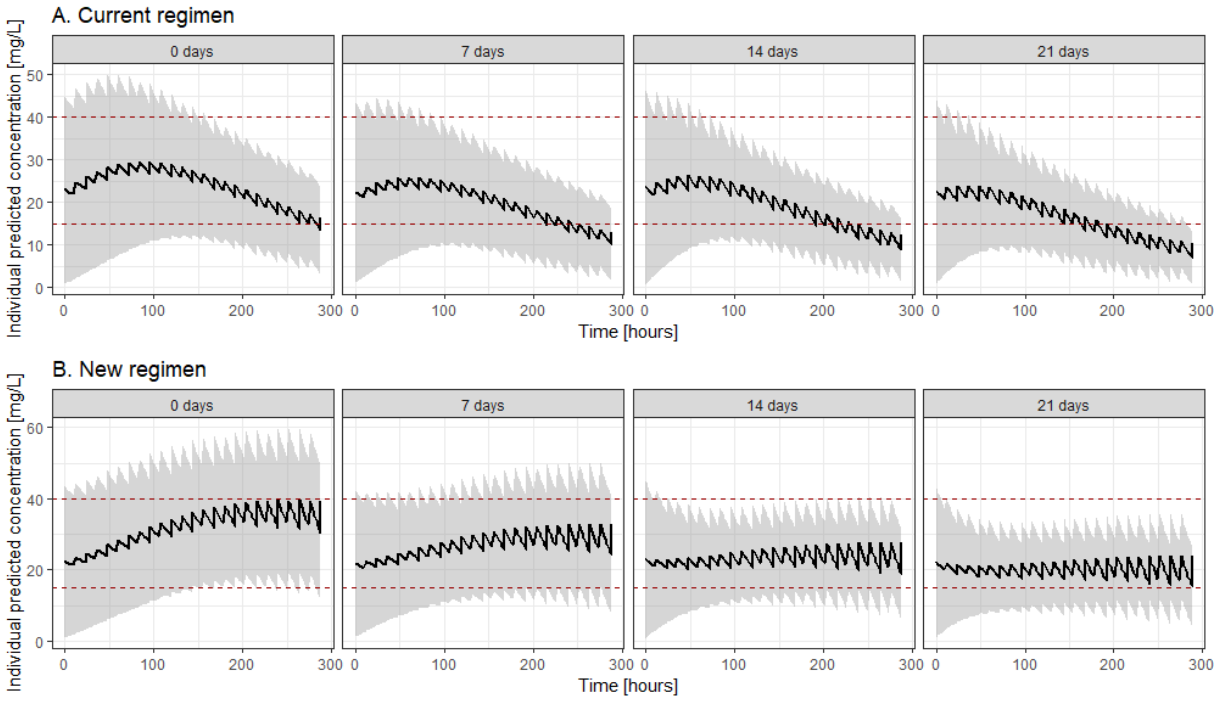

Figure 5. Simulated phenobarbital level *vs.* time. Phenobarbital levels are represented as median with 95% prediction intervals, for 1000 neonates with a birth bodyweight of 3.21 kg and a postnatal age at start of treatment of 0, 7, 14 and 21 days, with instantaneous onset of ECMO and phenobarbital therapy at time = 0. A. Currently recommended dosing regimen (loading dose, LD = 20 mg/kg; maintenance dose, MD = 5 mg/kg/day for neonates of PNA = 0 – 14 days and 6 mg/kg/day for neonates of PNA = 15 – 28 days divided in 2 daily doses); B. Newly proposed regimen (LD = 20 mg/kg, start with MD = 4 mg/kg/day with 0.25 mg/kg increase every 12 h during ECMO treatment).

In the **study 2**, BW was identified as the only statistically significant covariate for the Vd: Vd was 0.91 L at BW of 1 kg and for every additional kg it increased in 0.91 L. CL was 0.00563 L/h, and no statistically significant covariates were found for the CL of phenobarbital. The estimated values of PK parameters are presented in Table 2.

Table 2. Parameters of the final pop PK model of phenobarbital in neonates undergoing therapeutic hypothermia

Model parameter [units]	**Final parameter value (RSE)**

Fixed effects	
CL [L/h]	0.00563 (26%)
Vd = θBW * BW θBW [L/kg]	0.91 (5%)
Inter-individual variability	
CL	0.289 (68%)
Vd	0.0461 (28%)
Residual unexplained variability	
Additive	14.7 (17%)

Abbreviations: CL = clearance; Vd = volume of distribution; RSE = relative standard error; BW = body weight; θBW = increase in Vd per kg body weight

Diagnostics and validation of the final model showed that the data were described accurately. GOF shows no bias in description of individual and population predicted concentration of phenobarbital (Figure 6). Distribution of NPDE had a mean of 0.0684 and variance of 1.02. Neither mean nor variance significantly deviated from the expected values of 0 and 1, respectively. This also confirmed that the data were described accurately by the final model.

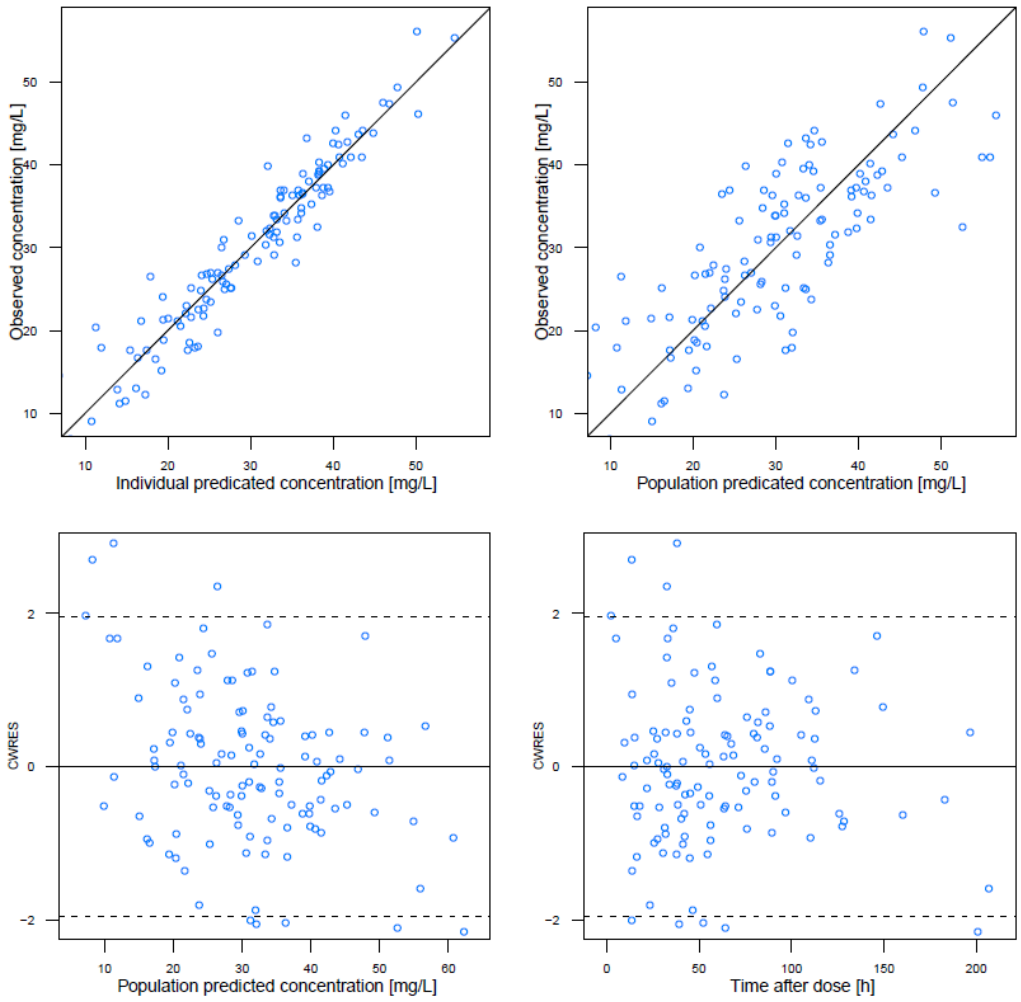

Figure 6. Goodness-of-fit plots of the final pharmacokinetic model for phenobarbital in newborns with asphyxia and hypoxic-ischemic encephalopathy treated with therapeutic hypothermia. CWRES = conditional weighted residuals.

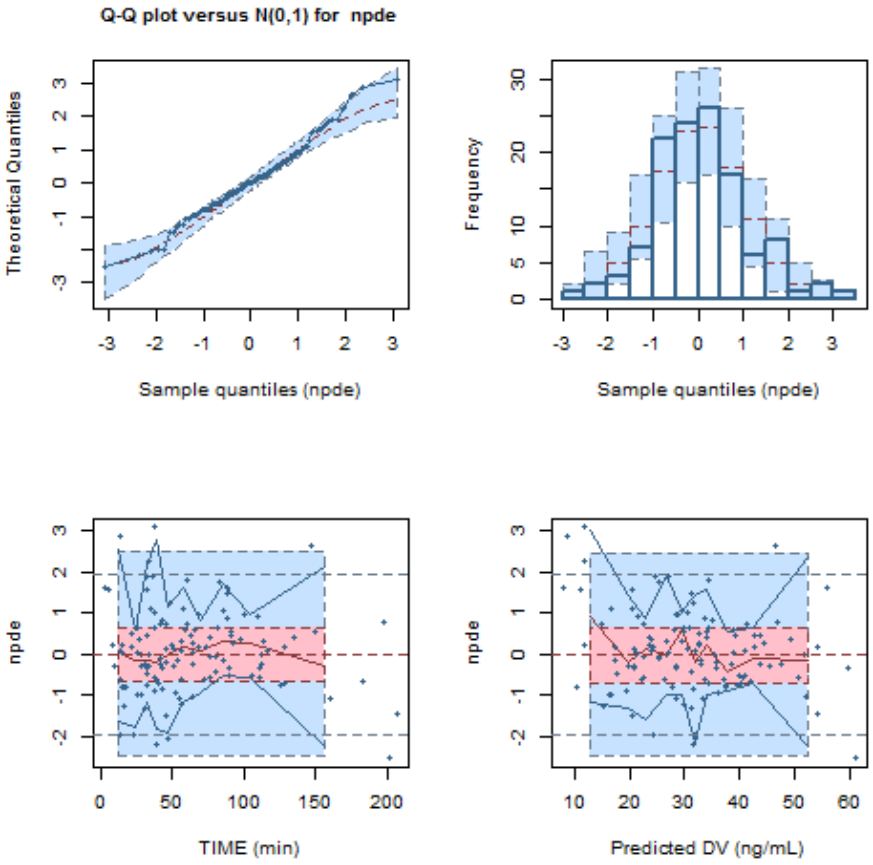

Figure 7. Visual output of the normalized prediction distribution error (NPDE) analysis for the pharmacokinetic model. Shown at the top are the QQ plot and histogram of the NPDEs in the overall dataset. The red dotted line and blue shaded areas show the expected trends and 95% confidence intervals of these trends, while the dark blue lines and bars show the observed NPDE distributions. At the bottom, the individual NPDE values for each observation are plotted versus time and versus the predicted concentrations with the symbols. The solid lines in the bottom graphs indicate the mean (red) and the 90% percentiles (blue) of the NPDEs, and the shaded areas are the simulated 90% confidence intervals of the NPDE median (red) and 90% percentiles (blue), while the dotted red and blue lines show the expected values for the median and 90% percentiles.

The obtained results of PK parameters were compared with the results of the studies evaluating phenobarbital PK in the past 20 years (32, 37-43) in Table 3. The reported CL values displayed significant variations, but the CL value estimated in this study was within the reported range. Therefore, it could not be concluded that CL of phenobarbital in neonates was linked to the treatment of therapeutic hypothermia.

Table 3. Overview of studies evaluating pharmacokinetic parameters of phenobarbital in newborns in the past 20 years

Population	Reference	Covariates found to be significant for CL	Covariates found to be significant for Vd	Phenobarbital administration route	Therapeutic hypothermia	Asphyxia + HIE	NMLE approach	CL (L/h) *	Vd (L)*
50 term neonates BW: 3.3 (2.8 –3.5) kg GA: 39 (38–40) weeks PNA: 2 (1−3) days	current analysis	BW	-	iv	yes	yes	yes	0.00563	3.03
19 term neonates BW: 2.3 ± 1.08 kg GA: 34 ± 4 weeks PNA: not reported	Touw *et al.* *(42)*	-	-	iv	no	no	no	0.01420	2.34
19 term neonates BW: 3.2 ± 0.64 kg GA: 39.6 ± 1.6 weeks PNA: not reported	Filippi *et al*. (39)	-	-	iv	yes	yes	no	0.02110	5.15
70 neonates and infants BW: 2.9 (0.67–5.2) kg GA: 38 (24–43) weeks PNA: 15.8 (1–73) days	Yukawa *et al.* (43)	BW, PNA, serum concentration of phenobarbital	BW	rect + po	no	no	yes	0.02020	3.33
31 neonates BW: 3.5 (2.15–4.92) GA: 39.9 (36.0–42.1) weeks PNA: not reported	Van den Broeck *et al.* *(38)*	BW	BW	iv	yes	yes	yes	0.01600	3.24

39 neonates BW: 3.49±0.58 kg GA: 39.5±1.7 weeks PNA: median 13.2, range not reported	Shelhaas *et al. (37)*	PNA, BW	BW	iv	yes (+ control group which was not cooled)	yes	yes	0.00560	3.06
48 neonates and infants BW: 4.26 (0.7–10) kg GA: 37.1 (27–42) weeks PNA: 26.8 (0–206) days	Marsot *et al. (40)*	BW	BW	iv + po	no	no	yes	0.01930	2.1
53 preterm and term neonates GA: 37 (24–42) weeks BW: 2.7 (0.45–4.5) kg PNA: 4.5 (0−22) days	Voller *et al. (32)*	birth BW, PNA	actual BW	iv + po	no	no	yes	0.00990	3.06
355 children (42.5% neonates, 7.6% >30 days of age and <2 years of age) BW: 4.9 (3.4 - 9.2) GA: 39 (35 - 40) weeks PNA: 102 (22-299) days	Moffett *et al. (41)*	FFM, PMA, SCR,	FFM, PNA	iv + po	no	no	yes	0.01010	2.24
40 term neonates BW: 3.26 ± 0.63 kg GA: 39.4 ± 1.3 weeks PNA: 4.8±5.7 h	Pokorná *et al. (35)*	-	-	iv	yes (+ control group which was not cooled)	yes	no	0.00693	1.71

* Values for Vd and CL are calculated for the typical individual in this study (BW=3.3 kg, PNA=2 days)

Pop PK = population pharmacokinetic; BW = body weight; PNA = postnatal age; GA = gestational age; PB = phenobarbital; FFM = fat-free mass; PMA = postmenstrual age; SCR = serum creatinine concentration; iv = intravenous; po = per oral; rect = rectal

In the **study 3**, in a one-compartment model, CL and Vd for a typical individual of the BW = 7.88 kg that was off CRRT were 1.09 L/h (RSE = 8%)) and 3.98 L (14%), respectively. BW was identified as a significant covariate for Vd and CL (parameter estimates presented in Table 4). In addition, CRRT treatment use increased Vd of meropenem approximately two times. Importantly, ECMO therapy did not induce any changes in Vd and CL of meropenem.

Table 4. Parameter estimates of the final model of meropenem in pediatric and neonatal patients undergoing ECMO

Parameter [units]	Final model (RSE %)	Bootstrap (95% CI)
Fixed effects		
CL [L/h] = CLp * (BW/7.88)		
CLp	1.09 (8%)	1.09 (0.98 – 1.21)
Vd [L] = Vp * (BW/7.88) * $(1+\theta CRRT)^{CRRT\_on}$		
Vp	3.98 (14%)	4.01 (2.22 – 7.30)
θCRRT	1.04 (76%)	1.06 (0.14 -2.20)
Inter-individual variability		
CL	0.0887 (48%)	0.0882 (0.0429 – 0.1510)
Vd	0.916 (68%)	0.800 (0.060 – 1.729)
Residual unexplained variability		
Proportional	0.17 (17%)	0.167 (0.119 – 0.225)

Abbreviations: RSE = relative standard error of the estimate; CL = clearance; CLp = population clearance value; Vd = volume of distribution; Vp = population volume of distribution value; CRRT_on = binary parameter indicating whether CRRT treatment is on (1) or off (0); θCRRT = increase in Vd when CRRT treatment is on

Diagnostics and validation of the final model showed that the data were described accurately. The parameters of the final model were estimated with an acceptable precision, with RSE values below 50%, except for θCRRT and IIV for Vd. Despite the elevated uncertainty in these estimated values, the decision was made to maintain the covariate relationship in the model, given its substantial clinical value, as per the consensus among clinicians. GOF shows no bias in description of individual and population predicted concentration of meropenem, apart from 4 outlier concentrations (Figure 8), which were much lower than the observed. Distribution of NPDE had a mean of –0.05 and variance of 1.007 (Figure 9). Neither mean nor variance significantly deviated from the expected values of 0 and 1, respectively. This also confirmed that the data were described accurately by the final model. Apart from Vd, the bootstrap results indicated the model is robust, as values obtained in this procedure were within 10% of the values estimated in the final model fit. Regarding Vd, the median from the bootstrap analysis shows only a 13% deviation from the final parameter estimate.

Additionally, the final parameter value falls comfortably within the 95% bootstrap interval, enhancing the confidence in the obtained estimate.

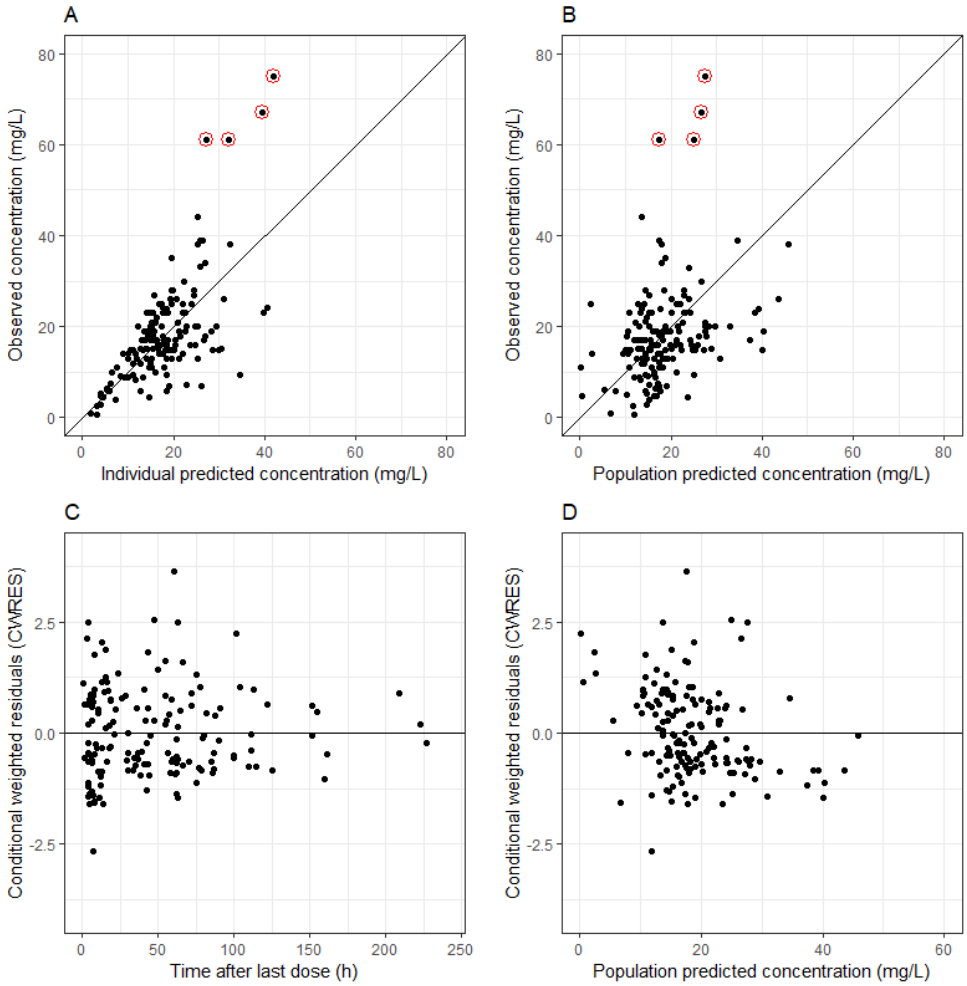

Figure 8. GOF plots of the final model of meropenem in neonatal and pediatric populations
CWRES = conditional weighted residuals

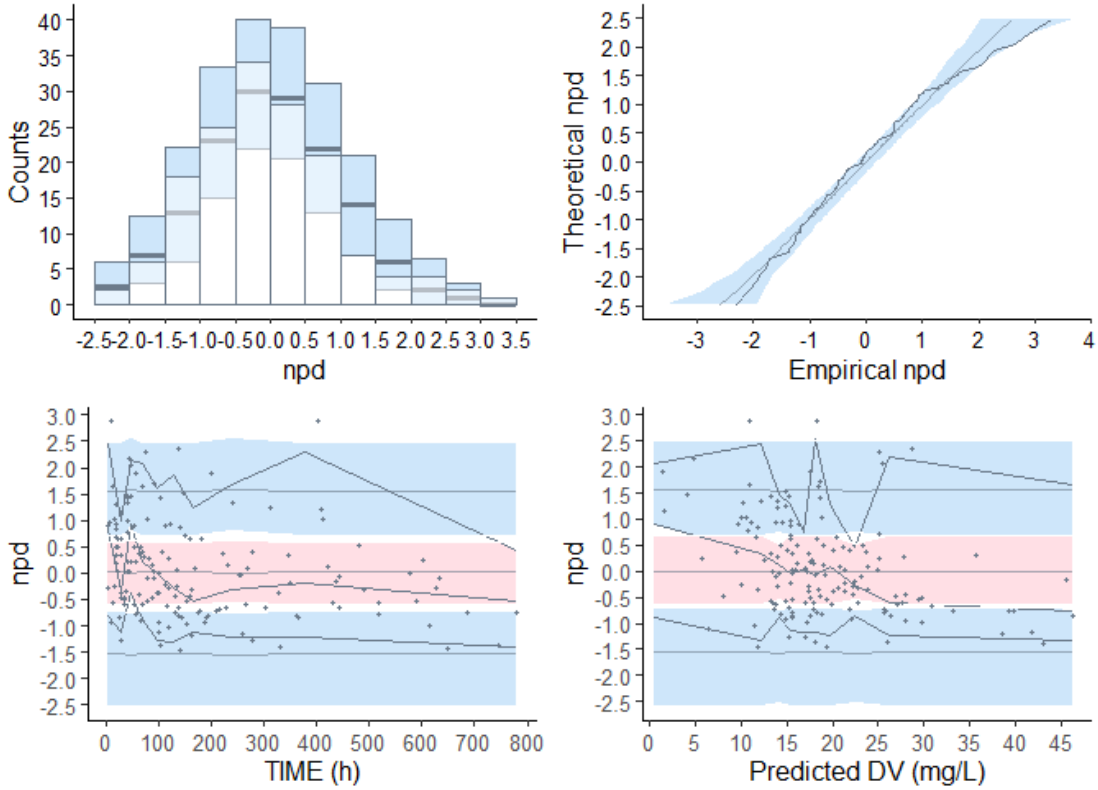

Figure 9. Visual output of the normalized prediction distribution error (NPDE) analysis. Shown at the top are the QQ plot and histogram of the NPDEs in the overall dataset. The red dotted line and blue shaded areas show the expected trends and 95% confidence intervals of these trends, while the dark blue lines and bars show the observed NPDE distributions. At the bottom, the individual NPDE values for each observation are plotted versus time and versus the predicted concentrations with the symbols. The solid lines in the bottom graphs indicate the mean (red) and the 90% percentiles (blue) of the NPDEs, and the shaded areas are the simulated 90% confidence intervals of the NPDE median (red) and 90% percentiles (blue), while the dotted red and blue lines show the expected values for the median and 90% percentiles.

Monte Carlo simulations showed that for 40% fT>MIC, all tested dosing regimens (infusion lasting 0.5 and 3 h for doses of 20 mg/kg and 40 mg/kg of meropenem every 8 h and continuous infusion of 60 and 120 mg/kg/day) provided high PTA for all MIC up to 4 mg/L, whereas for 100% fT>MIC PTA was achieved only for continuous infusion of 120 mg/kg/day for MIC = 0.5 mg/L. The results of Monte Carlo simulations are presented in Table 5 (40% fT>MIC) and 6 (100% fT>MIC). PTA higher than 90% are highlighted.

Table 5. Probability of target attainment for 40%T>MIC

	20 mg/kg 30 min q8h		20 mg/kg 3 h q8h		40 mg/kg 30 min q8h		40 mg/kg 3 h q8h		60 mg/kg cont.		120 mg/kg cont.	
MIC	CRRT=0	CRRT=1	CRRT=0	CRRT=1	CRRT=0	CRRT=1	CRRT=0	CRRT=1	CRRT=0	CRRT=1	CRRT=0	CRRT=1
0.5	93	98	98	99	95	98	98	99	100	100	100	100
1	91	97	97	99	93	98	98	99	100	100	100	100
2	87	96	95	99	90	98	97	99	100	100	100	100
4	80	93	92	98	87	96	95	99	100	100	100	100
8	55	64	71	78	79	81	82	85	99	99	100	100
16	17	28	35	42	55	65	69	70	45	53	69	69

Table 6. Probability of target attainment for 100%T>MIC

	20 mg/kg 30 min q8h		20 mg/kg 3 h q8h		40 mg/kg 30 min q8h		40 mg/kg 3 h q8h		60 mg/kg cont.		120 mg/kg cont.	
MIC	CRRT=0	CRRT=1	CRRT=0	CRRT=1	CRRT=0	CRRT=1	CRRT=0	CRRT=1	CRRT=0	CRRT=1	CRRT=0	CRRT=1
0.5	74	81	76	87	75	84	77	89	74	89	79	90
1	71	75	72	83	74	81	76	87	61	84	74	89
2	66	68	61	74	71	75	72	82	55	71	61	74
4	57	51	53	53	65	67	70	74	25	53	54	71
8	12	12	11	13	66	50	52	54	6	21	25	52
16	0	0	0	0	0	0	0	0	0	0	0	0

Pop PK studies in adult population

In **study 4**, a two-compartment model with log-normally distributed IIV on CL, V2, and Q (Figure 10) provided the best description of the observed vancomycin peritoneal and plasma concentrations. V1 corresponds to the peritoneal cavity and V2 to the remainder of the body. The best description of RUV for peritoneal and plasma concentrations was provided by proportional and combination residual error models, respectively. BW was found to be a significant covariate for V2, whereas perseverance of diuresis (vs. existence of oliguria, defined as urine output < 500 mL) and estimated glomerular filtration rate according to CKD-EPI (2009) equation (eGFR) were predictive covariates for CL of vancomycin. For a typical individual of BW of 75 kg, and eGFR of 6.76 mL/min with oliguria, V1, CL, V2, and Q are 2 L (volume of exchange), 0.192 L/h (RSE = 17%), 23.6 L (78%), and 0.544 L/h (16%), respectively. Additionally, the inter-occasional variability (IOV) on Q was also included into the model, as it significantly improved the model fit (Figure 11). Still, IOV was relatively small in comparison to IIV, indicating that the variability within patients on different occasions was smaller than variability between patients. Estimates of the final model with the corresponding bootstrap results are presented in Table 7.

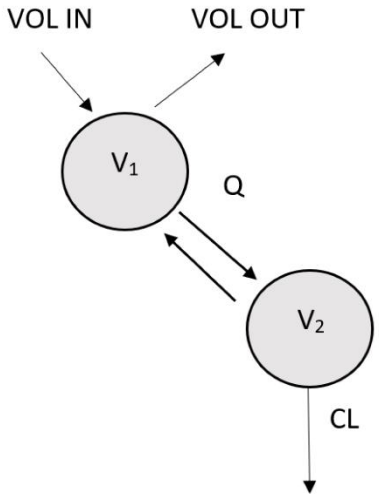

Figure 10. Schematic diagram of the final model of vancomycin in end stage renal disease patients receiving peritoneal dialysis. V1 = volume of peritoneal compartment, which represents peritoneal cavity; V2 = volume of central (systemic) compartment; CL = clearance; Q = intercompartmental clearance; VOL IN— infused peritoneal dialysate volume; VOL OUT—volume of dialysate that was removed out at the end of the dwell.

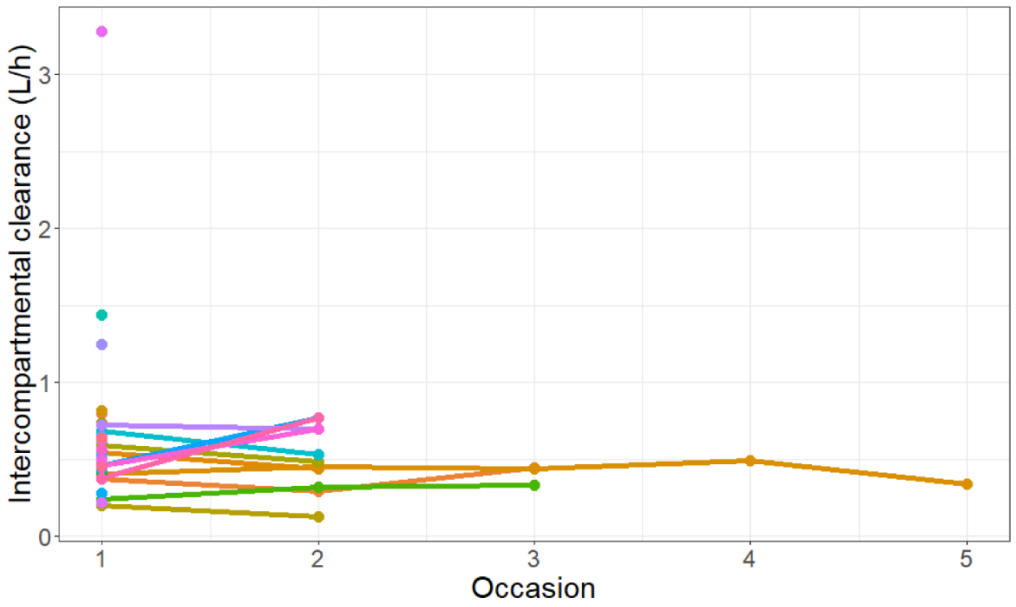

Figure 11. The values of inter-compartmental clearance for all included patients on different occasions. Different subjects are represented by different colors.

Structural parameters were estimated with acceptable precision, as RSE values generally were well below the limit of 50% with the exception for V2. The basic GOF plots for plasmatic concentrations (Figure 12) imply that the model describes the observed data accurately, apart from a small bias in plot of CWRES *vs.* predicted population concentrations. Additionally, no bias was observed in basic GOF plots for peritoneal concentrations (Figure 13), implying an accurate description of these data by the final model. Apart from V2, the bootstrap results indicated the model is robust, as values obtained in this procedure were within 10% of the values estimated in the final model fit. Regarding V2, the median from the bootstrap analysis shows only a 15% deviation from the final parameter estimate. Additionally, the final parameter value falls comfortably within the 95% bootstrap interval, enhancing the confidence in the obtained estimate.

The distribution of the NPDEs obtained with the final model for plasma concentrations had a mean of 0.1027 and variance of 0.848 and neither of these values deviated significantly from the expected values of 0 ($p = 0.254$) and 1 ($p = 0.253$), respectively. The distribution of NPDEs for peritoneal concentrations had a mean of 0.1228 and variance of 0.8438 and neither of these values deviated significantly from the expected values of 0 ($p = 0.381$) and 1 ($p = 0.8438$), respectively.

Table 7. Parameters of the final population PK model of vancomycin in patients treated with CAPD

Parameter [units]	Final model (RSE %)	Bootstrap
	Fixed effects	
V1 [L]	FIXED *	
Cl [L/h] = CLp * ((1 + θDIURES)* (eGFR/6.76))$^{DIURES>500}$		
CLp [L/h]	0.192 (17%)	0.186 (0.144-0.267)
θDIURES	1.26 (31%)	1.36 (0.50-2.25)
V2 [L] = V2p + θBWV * (BW/75)		
V2p [L]	23.6 (78%)	27.2 (1.68-65.3)
θBWV	50.9 (38%)	45.9 (9.6-76.0)
Q[L/h]	0.544 (16%)	0.53 (0.40-0.76)
	Inter-individual variability	
CL (%)	34.2 % (22%)	32.2% (16.0%-45.8%)
V2 (%)	30.3 % (21%)	29.2% (13.8%-40.4%)
Q (%)	50.7 (23%)	45.3% (20.1%-79.6%)
IOV on Q (%)	31% (37%)	30.1% (17.3%-51.7%)
	Residual unexplained variability	
Proportional, peritoneal concentration	0.091 (15%)	0.089 (0.064-0.146)
Additive, plasma concentration	4.72 (31%)	4.74 (1.38-7.11)
Proportional, plasma concentration	0.00604 (54%)	0.00649 (0.00045-0.01489)

* Fixed to the actual volume of peritoneal solution used (range 1 – 2 L)

Abbreviations: RSE = relative standard error of the estimate; Cl = clearance value; CLp = population clearance value; eGFR = estimated glomerular filtration rate; ΘDIURES = increase in CL when residual diuresis (DIURES) is preserved; RESDIU>500 = binary parameter designating DIURES is preserved (1) or not (0); V1 = volume of peritoneal compartment; V2 = individual volume of central (systemic) compartment value; V2 = population volume of central (systemic) compartment value; θBWV = increase in V2 per kg body weight.

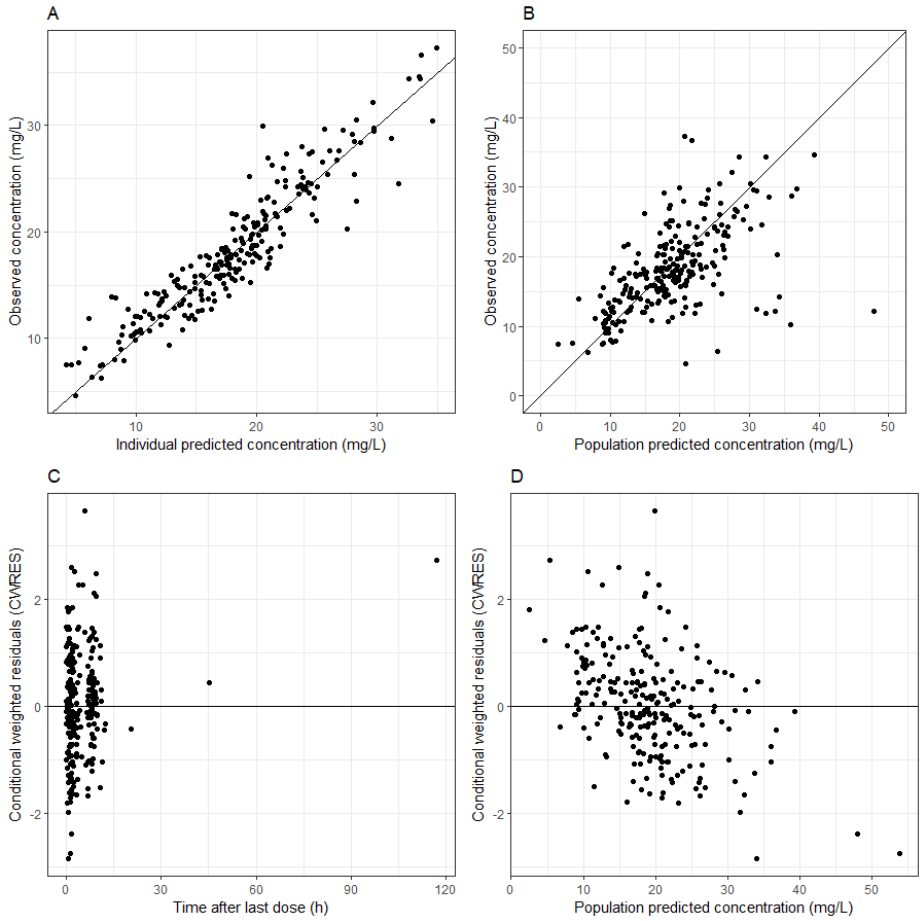

Figure 12. Goodness-of-fit plots for the final model for plasmatic vancomycin concentrations in patients receiving CAPD.
CWRES = Conditional weighted residuals

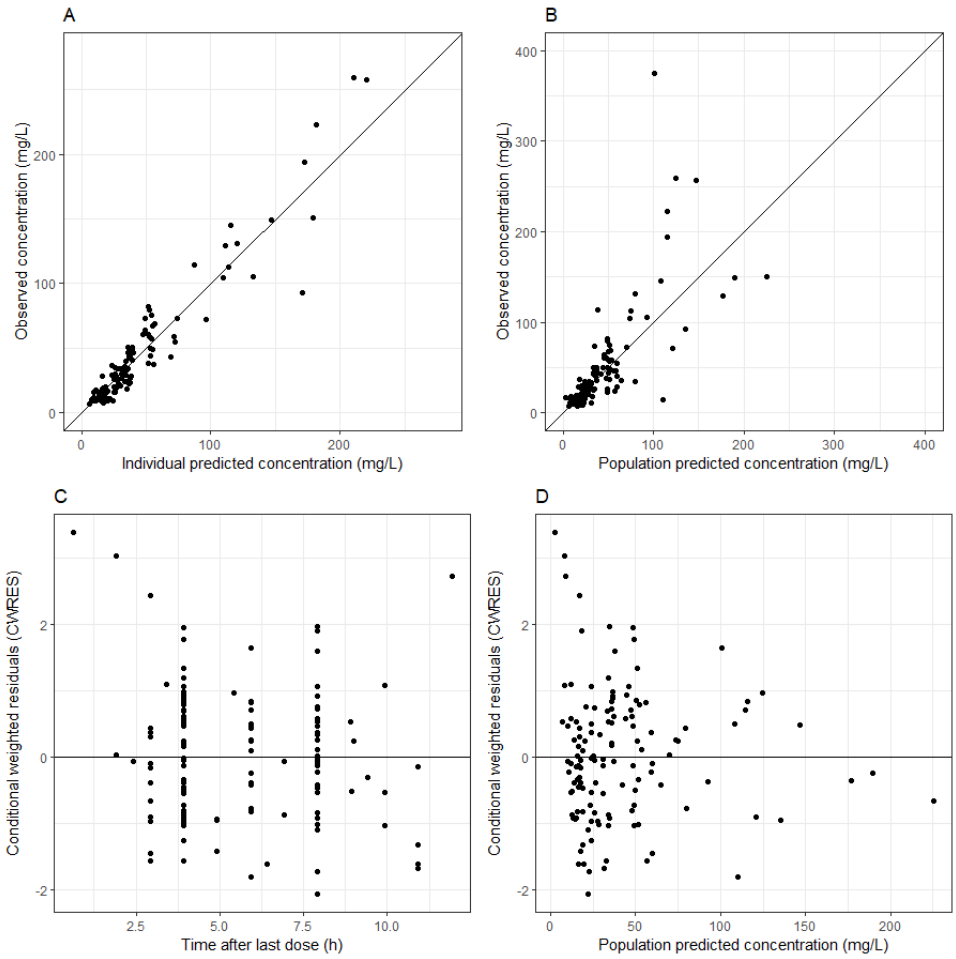

Figure 13. Goodness-of-fit plots for the final model for peritoneal vancomycin concentrations in patients receiving CAPD.
CWRES = Conditional weighted residuals

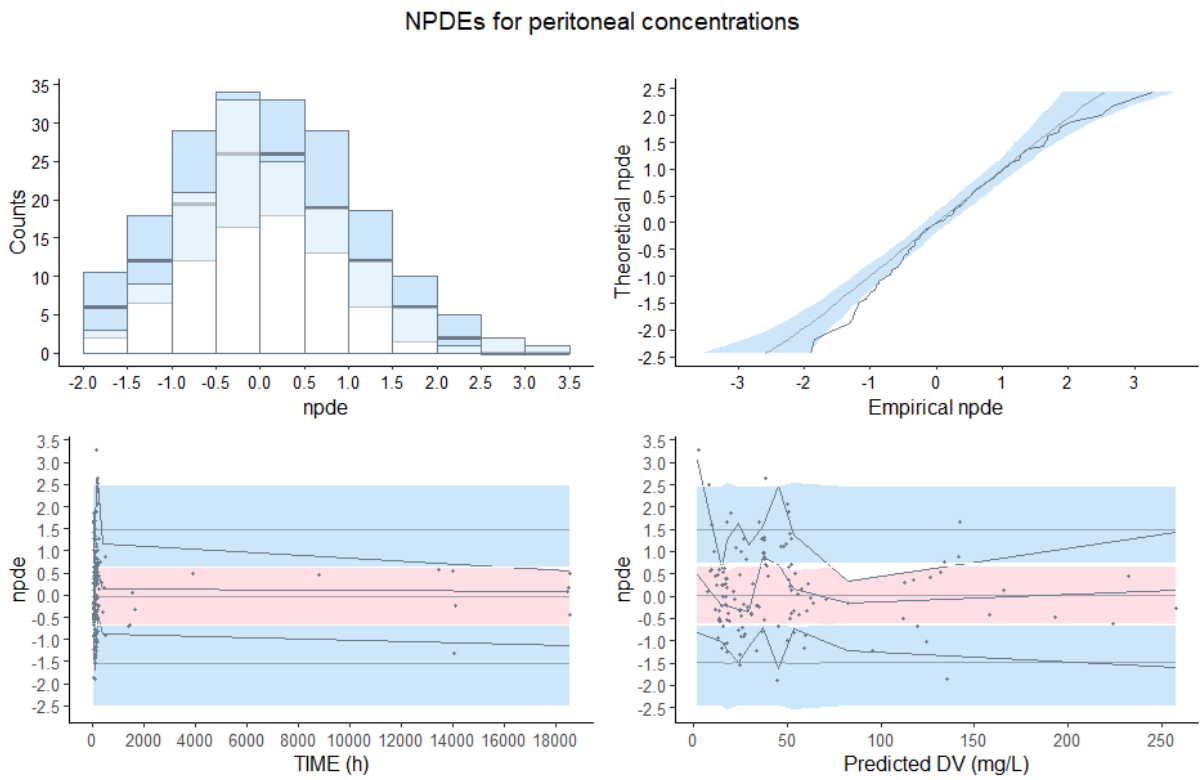

Figure 14. Normalized prediction distribution errors (NPDEs) for plasmatic vancomycin concentrations. Visual output of the normalized prediction distribution error (NPDE) analysis. Shown at the top are the QQ plot and histogram of the NPDEs in the overall dataset. The red dotted line and blue shaded areas show the expected trends and 95% confidence intervals of these trends, while the dark blue lines and bars show the observed NPDE distributions. At the bottom, the individual NPDE values for each observation are plotted versus time and versus the predicted concentrations with the symbols. The solid lines in the bottom graphs indicate the mean (red) and the 95% percentiles (blue) of the NPDEs, and the shaded areas are the simulated 95% confidence intervals of the NPDE median (red) and 95% percentiles (blue), while the dotted red and blue lines show the expected values for the median and 95% percentiles.

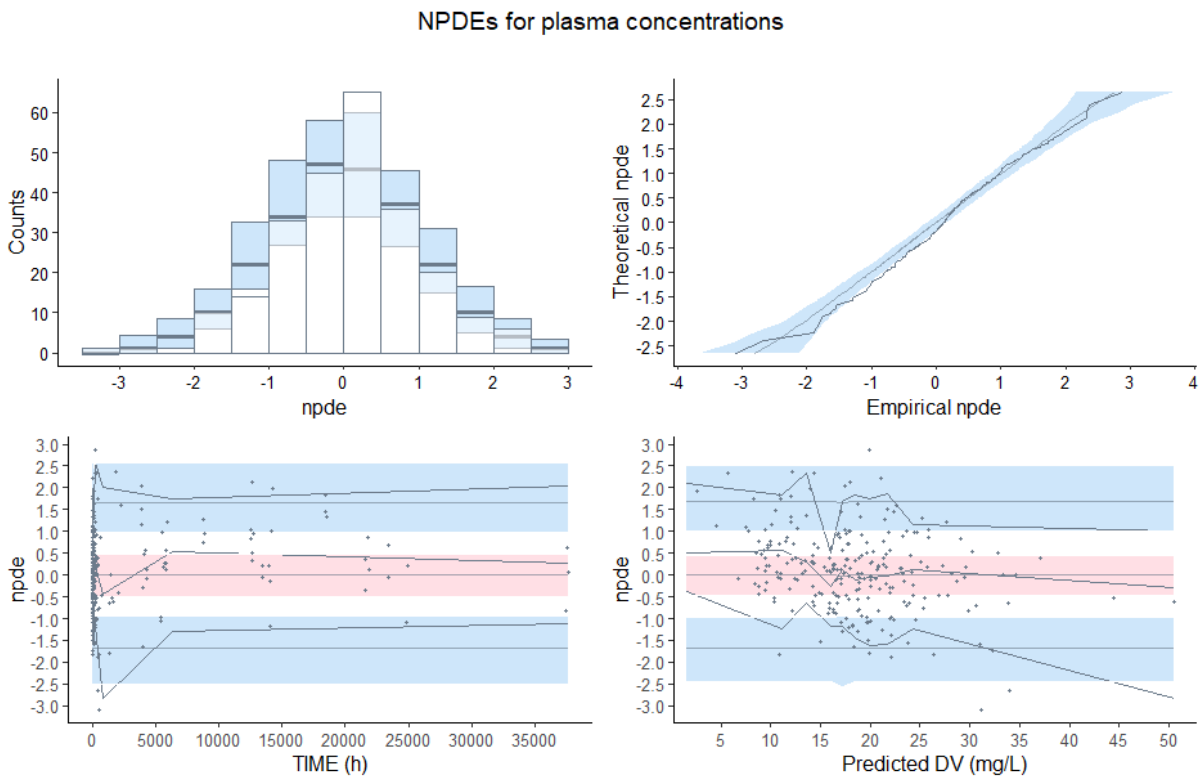

Figure 15. Normalized prediction distribution errors (NPDEs) for peritoneal vancomycin concentrations. Explanation of the legend is the same as for Figure 14.

Simulations were used to illustrate the implications of the pop PK model of vancomycin in patients with ESDR receiving peritoneal dialysis. Figure 16 depicts simulated plasmatic and peritoneal concentrations and calculated AUCs for peritoneal concentrations of vancomycin for a typical individual with BW of 75 kg and eGFR of 6.76 mL/min with preserved diuresis and oliguria for all dosing regimens recommended by ISPD. Simulations for patients with BW of 50 and 100 kg can be found in the corresponding publication (appendix 4).

(**A**) 30 mg/kg every 5 days, 2 L exchange, preserved diuresis, BW = 75 kg

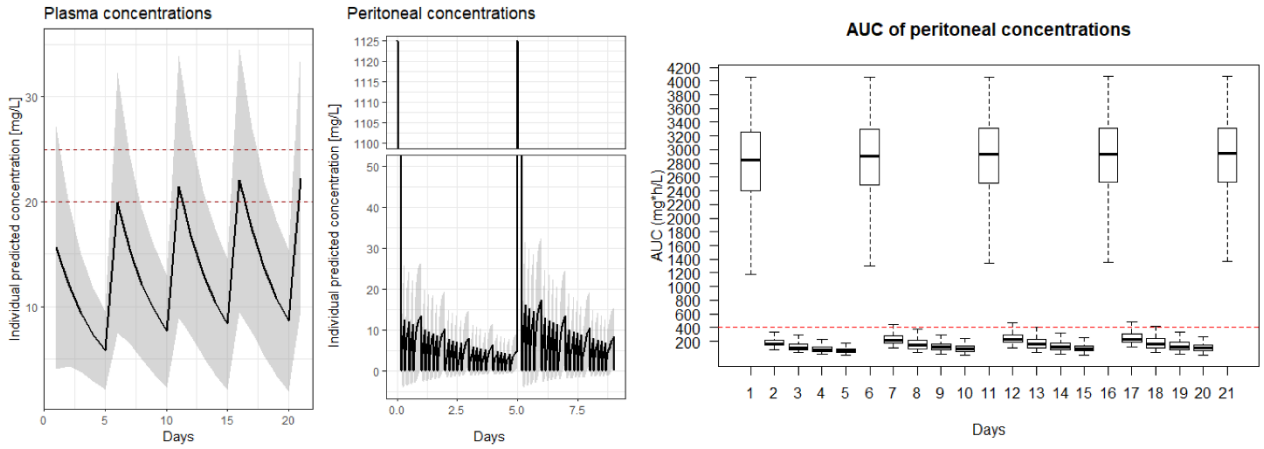

(**B**) 30 mg/kg every 5 days, 2 L exchanges, oliguria, BW = 75 kg

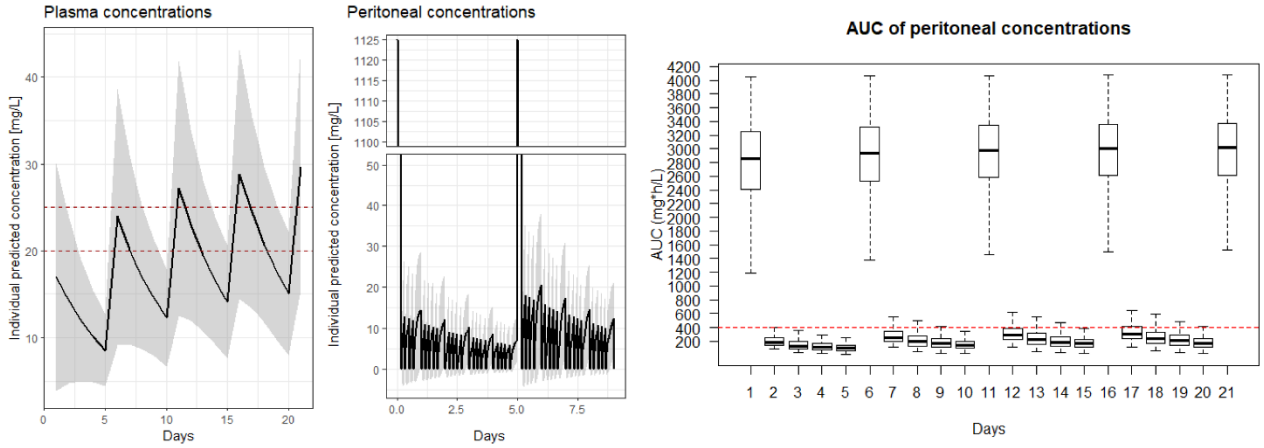

(**C**) 30 mg/kg every 7 days, 2 L exchanges, preserved diuresis, BW = 75 kg

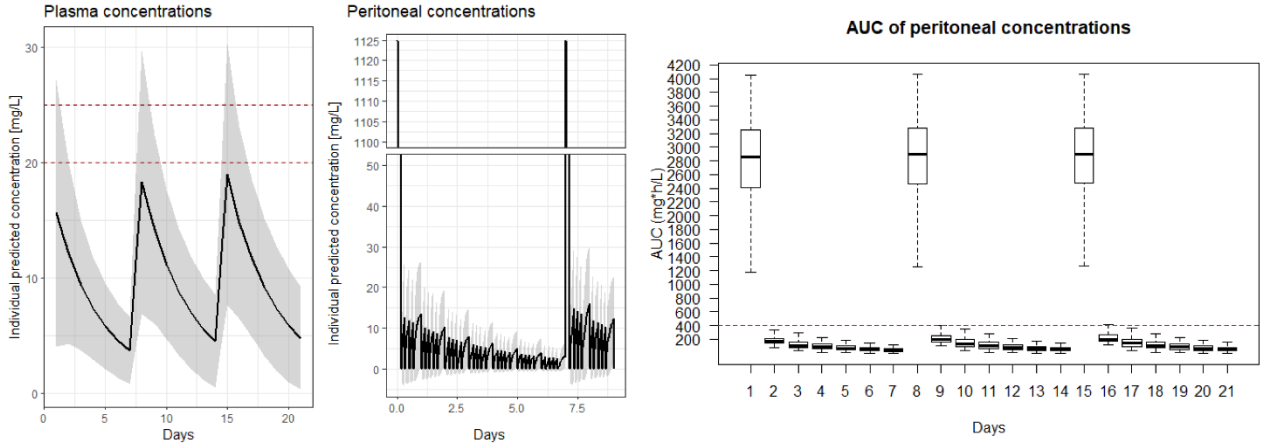

(**D**) 30 mg/kg every 7 days, 2 L exchanges, oliguria, BW = 75 kg

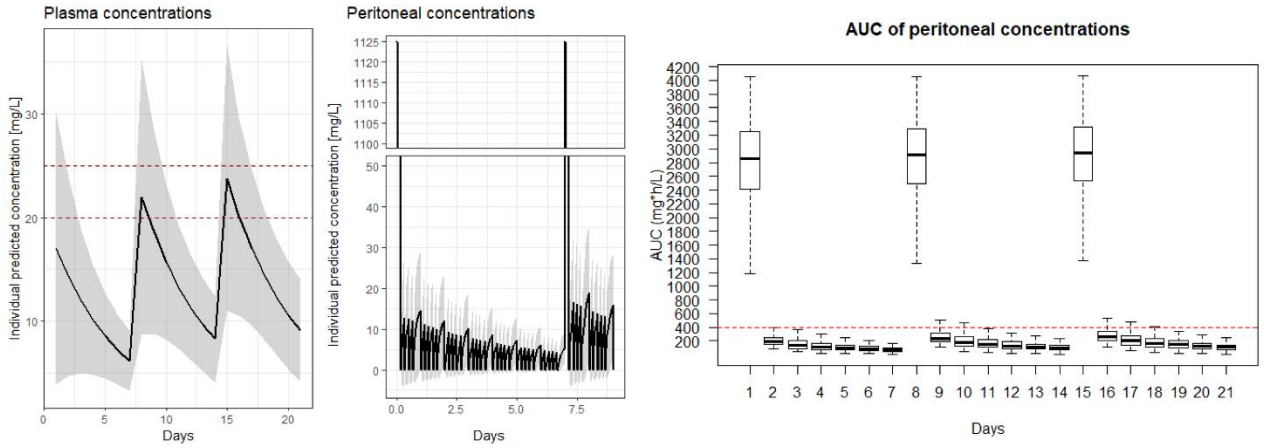

(**E**) LD = 25 mg/kg + MD = 25 mg/L in each dwell (2 L exchange), preserved diuresis, BW = 75 kg

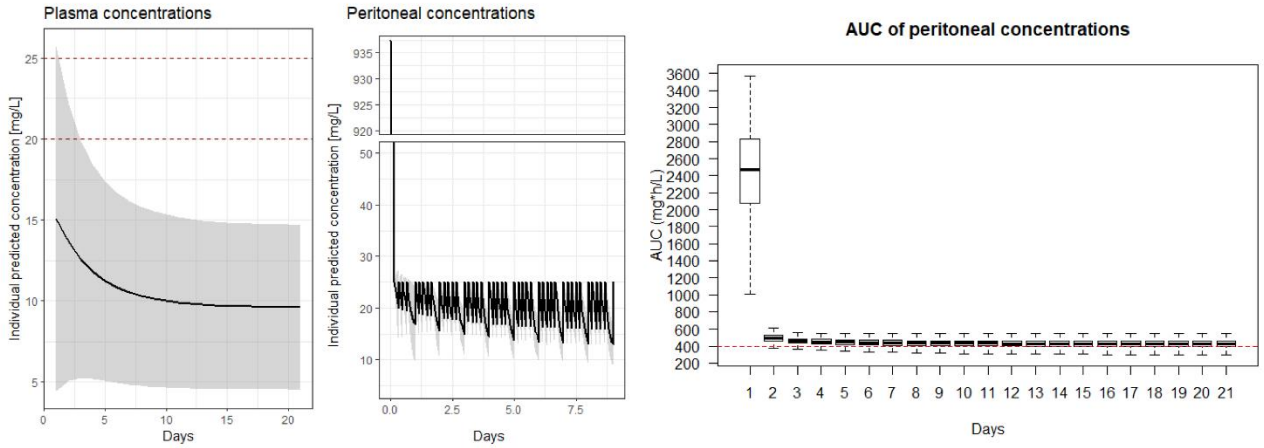

(**F**) LD = 25 mg/kg + MD = 25 mg/L in each dwell (2 L exchange), oliguria, BW = 75 kg

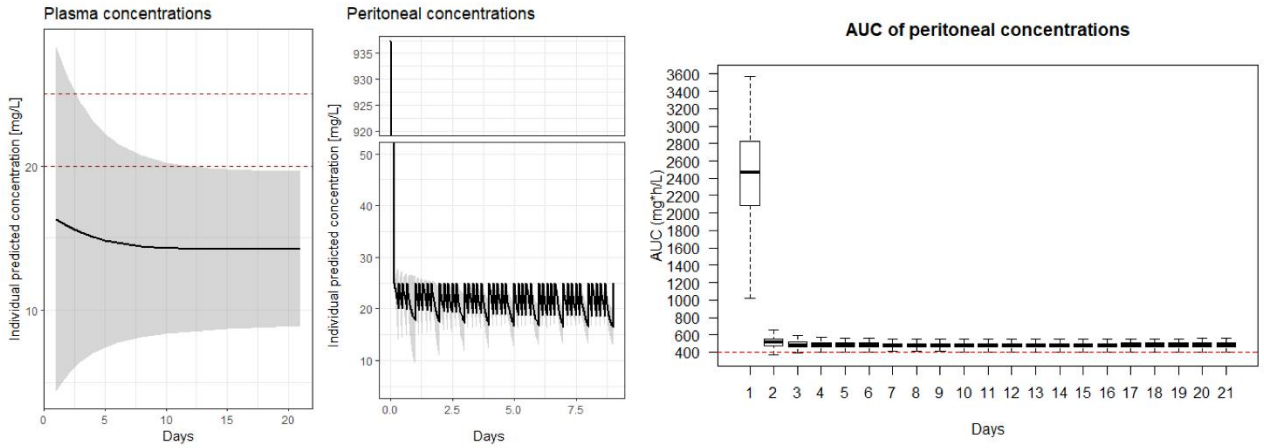

Figure 16. Simulations of vancomycin plasmatic and peritoneal concentrations upon recommended ISPD dosing regimens. AUC_{24} was calculated for a CAPD regimen consisting of 5 daily exchanges (i.e., 4 × 4 h and 1 × 8 h) in a patient with BW = 75 kg. When preserved diuresis was present, residual eGFR was set to 6.76 mL/min (median eGFR in the original dataset). In the left graphs, red lines

represent target plasma concentrations range, in the right graphs, red line represent target vancomycin AUC (i.e., 400 mg×h/L) that should be achieved for effective therapy. Abbreviations: AUC= area under the curve of peritoneal concentrations. LD = loading dose, MD = maintenance dose. Oliguria = urine output with less than 500 mL/day; Preserved diuresis = urine output with more than 500 mL/day. Medians of simulated concentrations are presented by solid lines; 95% confidence intervals of simulated concentrations are presented by shaded areas; AUC_{24} for 21-day-long treatment are presented with box plots with whiskers from minimum to maximum.

The intended exposure target of >400 mg×h/L in the peritoneum was not attained for the majority of the days during intermittent dosing. Additionally, treatment may only be marginally efficacious when recommended continuous dosing is employed in patients with preserved diuresis. Simulations clearly illustrate that, during continuous administration, a majority of patients would not reach the target therapeutic plasmatic level of 20–25 mg/L. This suggests a need for an increase in i.p. MD during continuous administration. Conversely, with intermittent dosing every 5 days in oliguric patients, a significant proportion of patients may already be overdosed after the second dose, even though insufficient exposure is achieved in the peritoneum. Based on the current model, we recommend an optimal dosing regimen (LD of 20 mg/kg followed by MD of 50 mg/kg in each subsequent dwell). This regimen aims to enhance intraperitoneal vancomycin exposure without overdosing patients with toxic plasma levels, as depicted in Figure 17. This figure shows vancomycin exposure in a patient with a median BW of 75 kg, simulations for patients with BW of 50 and 100 kg can be found in the corresponding publication (appendix 4).

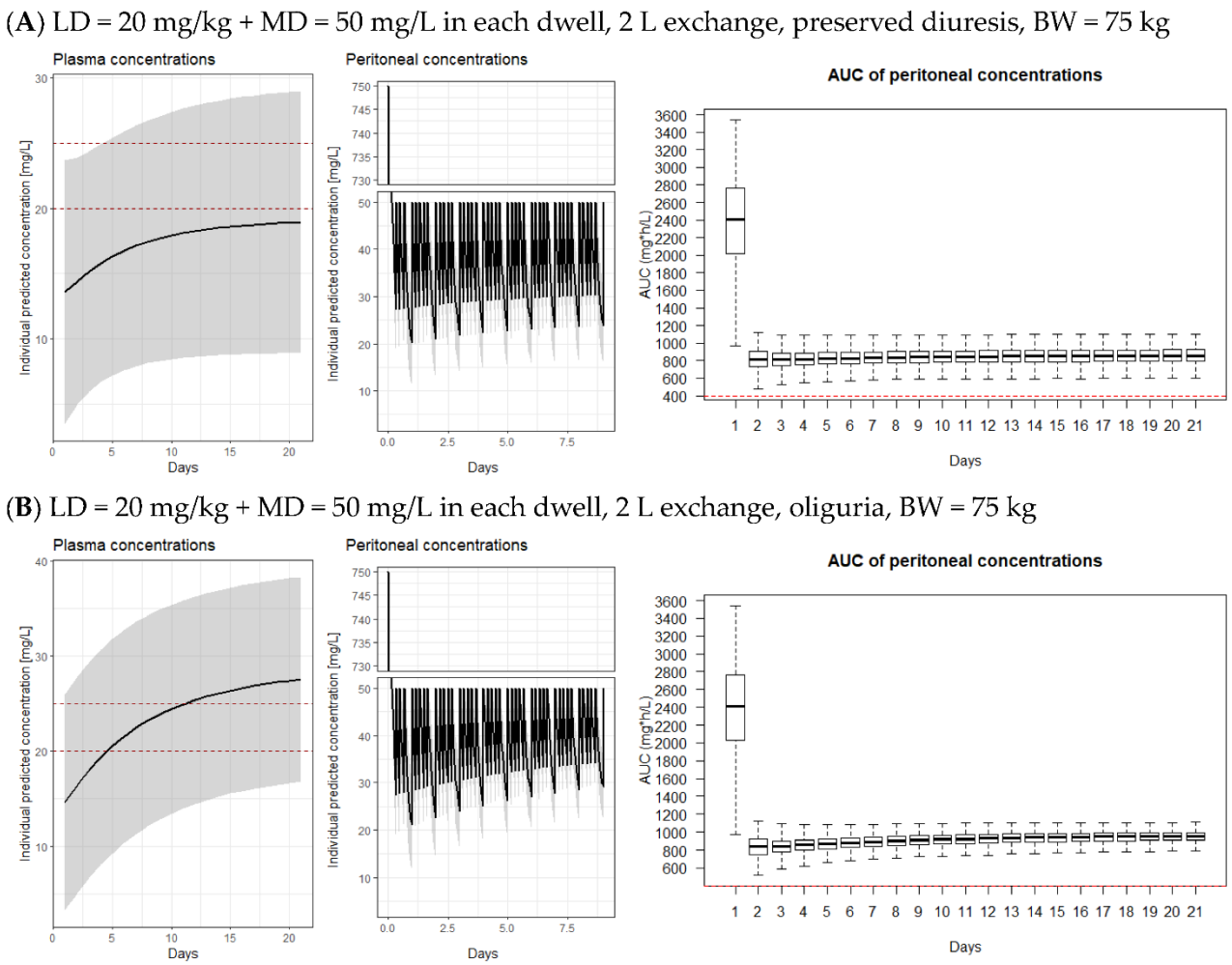

Figure 17. Newly proposed dosing regimen: vancomycin exposure in a patient with a median BW of 75 kg. A. patients with preserved diuresis B. patients with oliguria

Study 5 found that a one-compartment model with log-normally distributed IIV on CL Vd provided the best description of fondaparinux PK in ESRD patients. In the final model, CL and Vd were estimated to be 0.0529 L/h and 5.55 L, respectively. HF hemodialysis increased fondaparinux CL 2.26-fold, compared to the conditions with LF hemodialysis, peritoneal dialysis, or no hemodialysis ($p < 0.001$). There was no difference between CL during LF hemodialysis and no hemodialysis. TPE increased fondaparinux CL 7.06 times ($p < 0.001$). However, the RSE value for this parameter of 96%, implied that the uncertainty of this parameter was too high to be reliable. Estimated parameters of the final model are given in Table 8.

Table 8. Parameter estimates of the final model

Parameter [units]	Final model (RSE %)
Fixed effects	
CL [L/h] = CLp * (1 + θTYPEDIAL)	
CLp [L/h]	0.0528 (12%)
θTYPEDIAL	1.3 (34%)
V [L]	5.56 (13%)
SLOPE	1.18 FIX
Inter-individual variability	
CL (%)	31.9 (15%)
Vc (%)	38.5 (19%)
Residual unexplained variability	
Additive	1.83 (17%)

Abbreviations: RSE = relative standard error of the estimate; CL = clearance; CL = population clearance value; θTYPEDIAL = binary parameter designating hemodialysis is high-flux (1) or low-flux (2); V = population of volume of distribution value; SLOPE = parameter for the correlation between fondaparinux concentration and anti-Xa activity

Parameters of the final were accurately described; RSE for all parameters were below 50%. GOF plots did not show any bias (Figure 18). Jackknife analysis did not identify any individual having a large influence on the parameter estimates. NPDE analysis (Figure 19) also supported the findings of the aforementioned validation procedures. The distribution of the NPDEs obtained for the final model had a mean of 0.1247 and variance of 0.9785; neither mean nor variance deviated significantly from the expected values of 0 ($p = 0.185$) and 1 ($p = 0.907$), respectively.

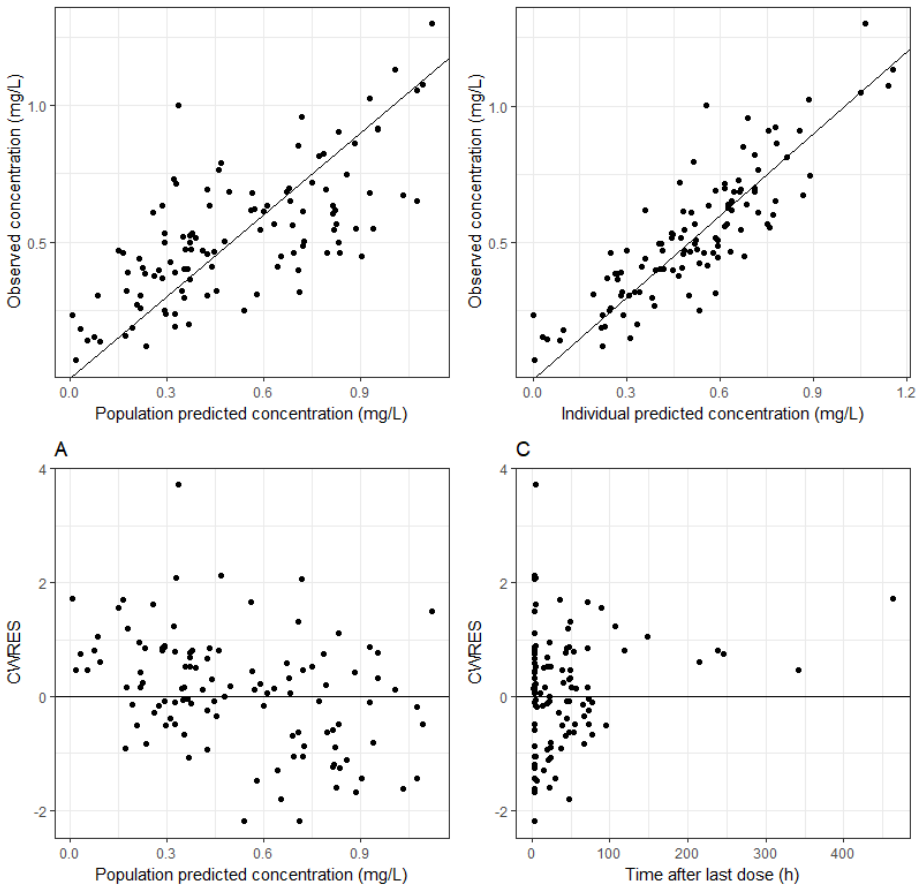

Figure 18. Basic goodness of fit plots of fondaparinux in end stage renal disease patients.
CWRES = Conditional weighted residuals

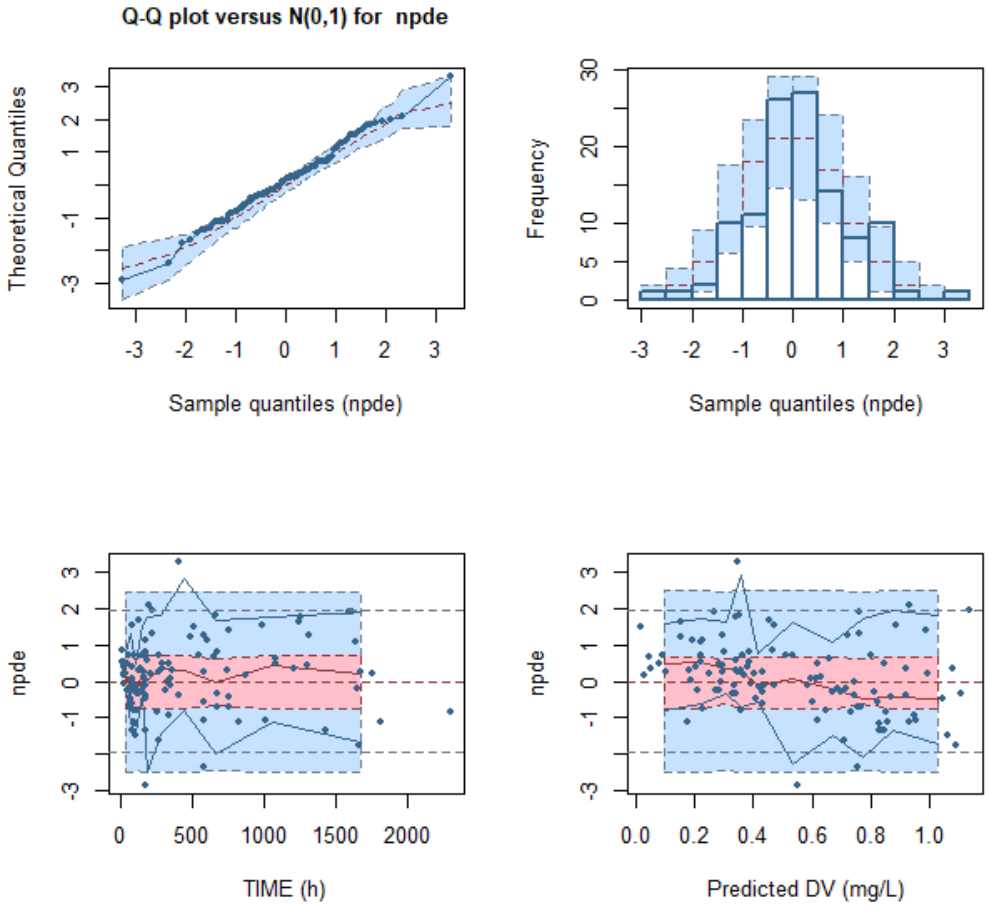

Figure 19. Normalized prediction distribution errors (NPDEs). Visual output of the normalized prediction distribution error (NPDE) analysis. Shown at the top are the QQ plot and histogram of the NPDEs in the overall dataset. The red dotted line and blue shaded areas show the expected trends and 95% confidence intervals of these trends, while the dark blue lines and bars show the observed NPDE distributions. At the bottom, the individual NPDE values for each observation are plotted versus time and versus the predicted concentrations with the symbols. The solid lines in the bottom graphs indicate the mean (red) and the 95% percentiles (blue) of the NPDEs, and the shaded areas are the simulated 95% confidence intervals of the NPDE median (red) and 95% percentiles (blue), while the dotted red and blue lines show the expected values for the median and 95% percentiles.

Simulations were performed to illustrate the findings of this study. As depicted on Figure 20, the simulated median post-dialysis anti-Xa levels for HF and LF hemodialysis are 0.72 IU/mL and 0.98 IU/mL, respectively. These values of anti-Xa activity correspond to the levels achieved at steady state after hemodialysis after the 2nd shorter dosing interval (48 h) in the week. Median pre-dialysis anti-Xa levels for HF and LF hemodialysis are 0.40 IU/mL and 0.55 IU/mL, respectively. These values correspond to through anti-Xa activity levels reached at steady state before hemodialysis after the longer dosing interval (72 h) in the week. The calculated inter-dialytic half-life (half-life for patients

undergoing LF hemodialysis and peritoneal dialysis) is 73 h, whereas calculated half-life during HF hemodialysis is 32 h. Finally, based on simulations, it can be concluded that the treatment including LD of 5 mg reaches steady-state anti-Xa activity levels in the first week of fondaparinux therapy, while it is reached in the second week without LD.

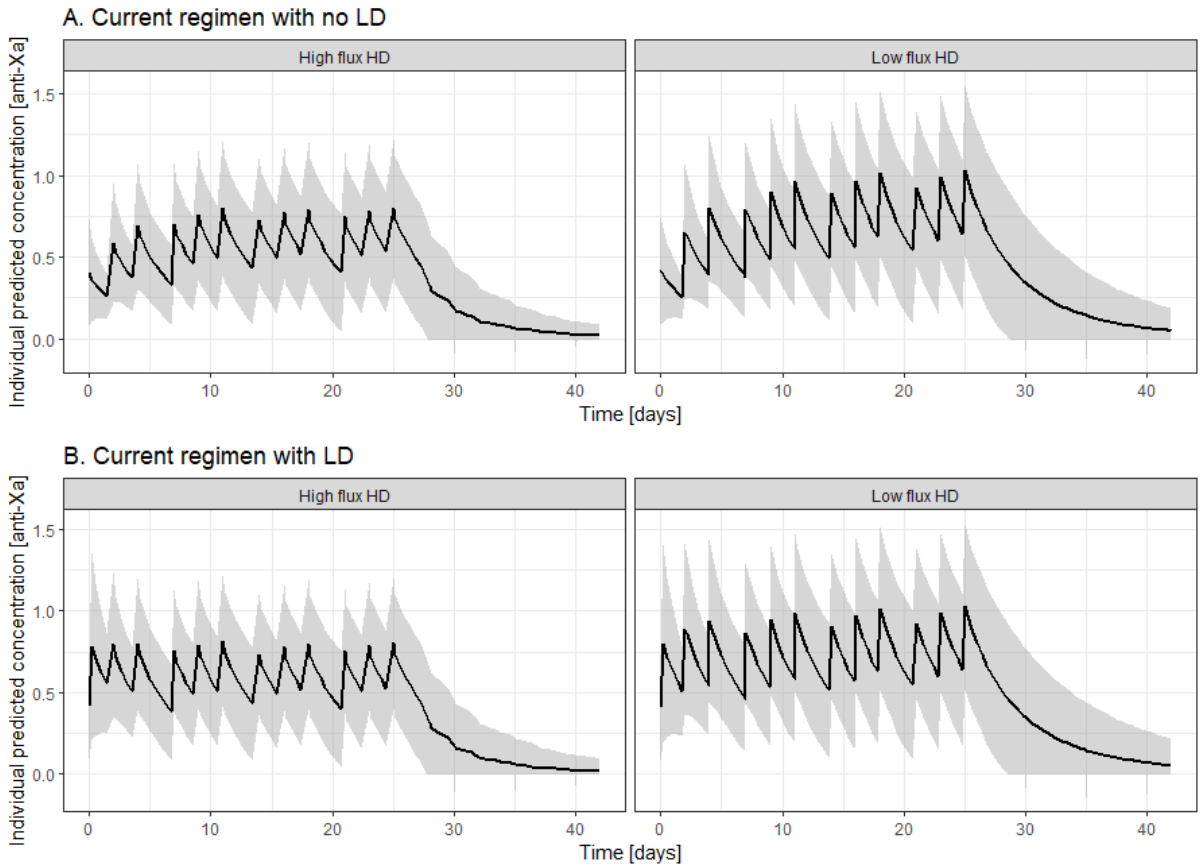

Figure 20. Simulated fondaparinux anti-Xa levels vs. time. Levels are represented as median with 95% prediction intervals, for 1000 patients: A. Dosing regimen consisting of a loading dose of 2.5 mg and a maintenance dose of 2.5 mg administered 3 times a week; B. Dosing regimen consisting of a loading dose of 5 mg and a maintenance dose of 2.5 mg administered 3 times a week

Study 6 found a two-compartment model to provide the best description of ampicillin distribution with IIV terms on V1, V2, Q and CL. A proportional error model provided the most accurate description of RUV. EGFR was found to be a significant covariate for ampicillin CL, and BW served as predictive covariate for both V1 and V2. The estimated pop PK parameters and corresponding bootstrap results for the final ampicillin model are presented in Table 9. The equations describing relationship between ampicillin PK parameters and their covariates are given in the following manner:

$\log(CL) = \log(CLp) + \beta\_CL\_eGFR \times eGFR + \eta\_CL$

$\log(V1) = \log(V1p) + \beta\_V1\_BW \times BW + \eta\_V1$

Log (Q) = log (Qp) + η_Q
Log (V2) = log (V2p) + β_V2_BW×BW + η_V2

Table 9. Estimates of final population pharmacokinetics model of ampicillin

	Final model	**Bootstrap results**	
Parameter	**Estimate (RSE)**	**Median**	**95% CI**
	Fixed effects		
CLp (L/h)	0.065 (20.5)	0.066	0.044-0.108
β_CL_eGFR	0.57 (23.7)	0.55	0.224-0.823
V1p (L)	2.69 (40.5)	2.38	0.947-5.641
β_V1_BW	0.015 (30.4)	0.0165	0.007-0.027
Qp (L/h)	0.19 (8.34)	0.19	0.161-0.223
V2p (L)	3.24 (52.3)	2.85	0.809-8.668
β_V2_BW	0.016 (41.0)	0.018	0.003-0.034
	Interindividual variability		
CL	0.31 (14.3)	0.28	0.165-0.378
V1	0.27 (22.2)	0.27	0.111-0.383
Q	0.24 (25.2)	0.20	0.05-0.382
V2	0.35 (24.8)	0.35	0.138-0.688
	Residual unexplained variability		
Proportional	0.14 (5.75)	0.13	0.10-0.175

Abbreviations: V1p = population value of volume of central compartment; V2p = population value of volume of peripheral compartment; CLp = population value of clearance; β_CL_eGFR = increase in CL per mL/s/1.73 m^2; BW = body weight; Q = population value of inter-compartmental clearance; β_V1_BW= increase in V1 per kg BW; β_V2_BW= increase in V2 per kg BW

Diagnostics and validation procedures did not identify any major bias in GOF, NPDE and VPC (Figure 21) of the final model.

Monte Carlo simulations were performed and time to achieve PTA>95% for various PK/PD targets (50% and 100%fT>MIC), for different MIC values and different eGFR values. The results are presented in Table 10. As it can be seen from this table, for 50% fT>MIC for MIC = 8 mg/L, dose of 2000 mg of ampicillin administered before the surgery is not sufficient if the CBP operation lasts longer than 430 min, 320 min, 220 min and 140 min in patients with moderate to severe renal impairment, in patients with mild renal impairment, in patients with normal renal function and in patients with an increased eGFR, respectively. In that case, an additional dose (1000 mg i.v.) should be administered.

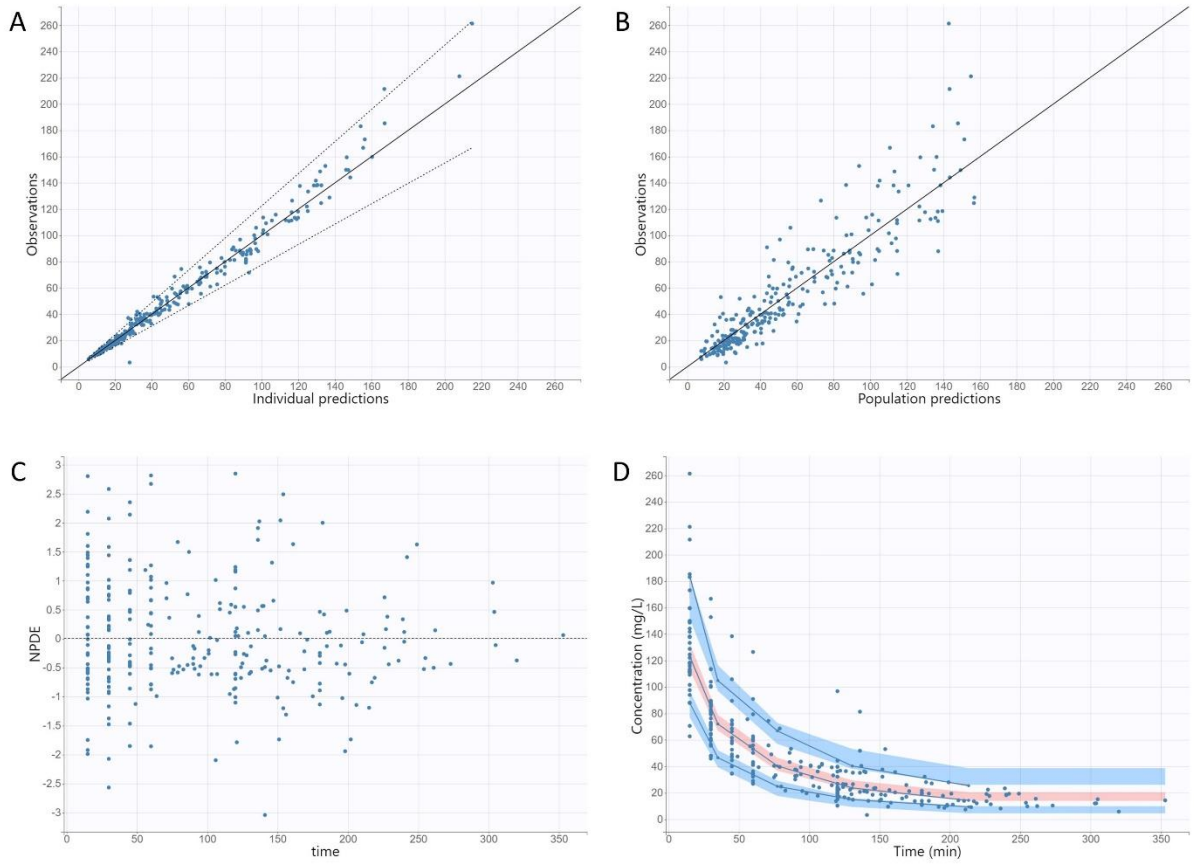

Figure 21. Goodness-of fit plots obtained from the final population pharmacokinetic model for ampicillin (A) Individual predicted concentrations vs. observed concentrations and (B) population predicted concentrations vs. observed concentrations; (C) Normalized prediction distribution errors (NPDE) vs. time after dose. (D) Visual predictive check (shaded areas) and observed data (circles) for concentrations vs. time for the final model. Solid blue lines represent the 10th, 50th, and 90th

percentiles of the observed data. Shaded regions represent 90% confidence interval around the 90th (above blue region), 50th (pink region), and 10th (below blue region) percentile of the simulated data.

Table 10. The time for which the PTA ≥ 95% was achieved for various PK/PD targets, for different MIC values and different eGFR values

eGFR	**<1 mL/s/1.73 m^2**	**1-1.5 mL/s/1.73 m^2**	**1.5-2.17 mL/s/1.73 m^2**	**>2.17 mL/s/1.73 m^2**
		fT>MIC = 50%		
MIC = 2 mg/L	>700 min	660 min	520 min	420 min
MIC = 8 mg/L	430 min	320 min	220 min	140 min
		fT>MIC = 100%		
MIC = 2 mg/L	>350 min	330 min	260 min	210 min
MIC = 8 mg/L	215 min	160 min	110 min	70 min

Abbreviations: eGFR = estimated glomerular filtration rate; MIC = minimal inhibitory concentration times rounded to nearest lower 5 min values

Study 7 found a two-compartment model to provide the best description of cefazolin distribution with IIV terms on V1, V2, Q and CL. A proportional error model provided the most accurate description of RUV. EGFR, BSA and MiECC/ECC use were found to be significant covariates for cefazolin CL, V1 and V2, respectively. The estimated pop PK parameters and corresponding bootstrap results for the final cefazolin model are presented in Table 9. The equations describing relationship between cefazolin PK parameters and their covariates are given:

$\log(CL) = \log(CLp) + \beta\_CL\_eGFR \times eGFR + \eta\_CL$

$\log(V1) = \log(V1p) + \beta\_V1\_BSA \times BSA + \eta\_V1$

$\log(Q) = \log(Qp) + \eta\_Q$

$\log(V2) = \log(V2p) + \beta\_V2\_MECC^{MECC} + \beta\_V2\_ECC^{ECC} + \eta\_V2$

Table 11. Estimated parameters of the final pop PK model of cefazolin in patients undergoing ECC during cardiac surgery

Parameter [units]	Final model (RSE %)	Bootstrap	
Fixed effects		**Median**	**95% CI**
CLp (L/h)	0.045 (21.7)	0.045	0.022-0.061
β_CL_eGFR	0.49 (24.5)	0.49	0.34-0.76
V1p (L)	4.91 (47.6)	3.87	0.76-10.20
β_V1_BSA	0.51 (44.8)	0.62	0.19-1.32
Qp (L/h)	0.28 (17.7)	0.30	0.15-0.44
V2p (L)	22.07 (18.2)	22.52	15.50-40.89
β_V2_MiECC	−0.79 (29.8)	−0.79	−1.33-(−0.20)
β_V2_ECC	−0.77 (32.2)	−0.74	−1.29-(−0.24)
Inter-individual variability			
CL	0.35	0.33	0.21-0.48
V1	0.10	0.18	0.08-0.32
Q	0.77	0.66	0.33-0.94
V2	0.58	0.52	0.17-0.76
Residual variability			
Proportional	0.16	0.15	0.14-0.17

Abbreviations: V1p = population value of volume of central compartment; V2p = population value of volume of peripheral compartment; CL = population value of clearance; β_CL_eGFR = increase in CL per mL/s/1.73 m^2; BSA = body surface area estimated according to DuBois formula; Q = population value of inter-compartmental clearance; β_V1_BSA = increase in V1 per m^2 BSA; β_V2_MiECC = decrease in V2 (L) with inclusion of minimally invasive extracorporeal circulation (MiECC); β_V2_ECC = decrease in V2 (L) with inclusion of ECC

Diagnostics and validation procedures did not identify any major bias in GOF and NPDE (Figure 22 and 23) of the final model.

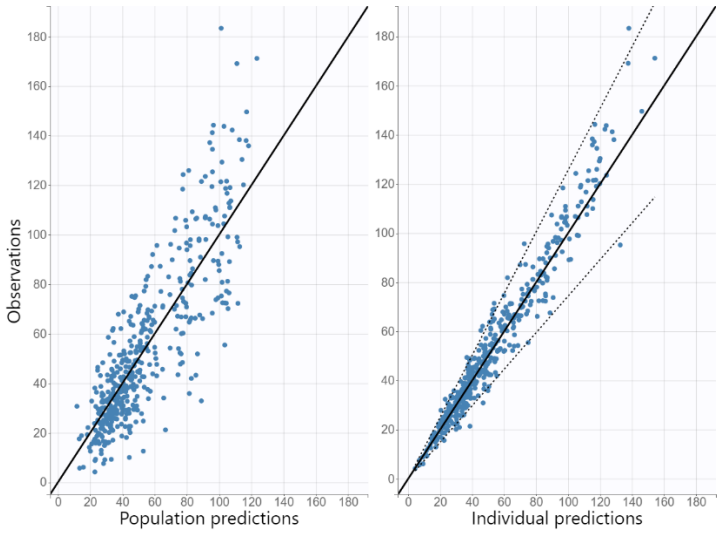

Figure 22. Goodness-of fit plots for the final population pharmacokinetic model for cefazolin: population and individual predicted concentrations vs. observed concentrations.

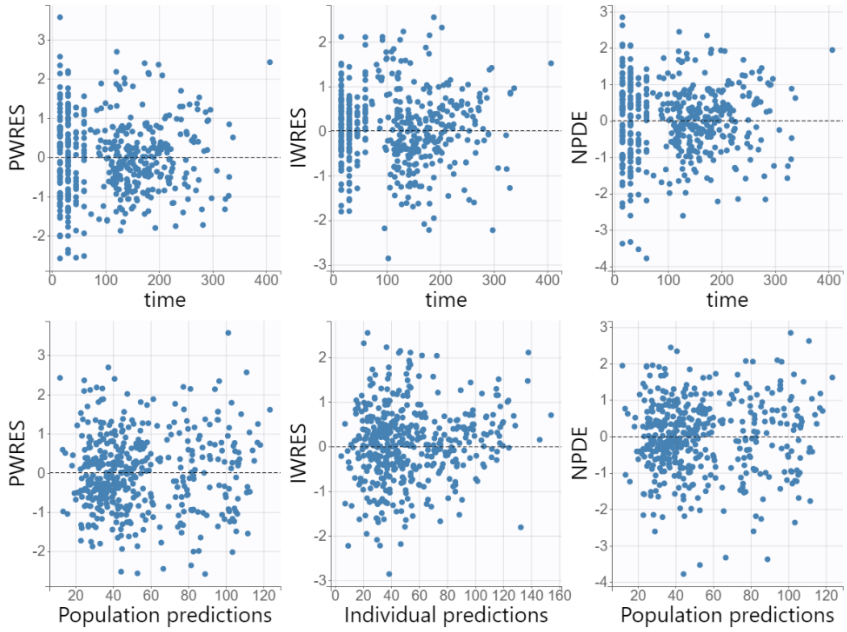

Figure 23. Goodness-of fit plots for the final population pharmacokinetic model for cefazolin: PWRES = population-weighted residuals, IWRES = individual-weighted residuals; NPDE = normalized prediction distribution errors

Monte Carlo simulations were used to predict PTA for cefazolin during 407 min, as this was the length of cefazolin administration. 500 simulations were performed for patients with various

functional renal statuses (eGFR < 1 mL/s, 1–2.17 mL/s and >2.17 mL/s) in the distribution corresponding to the real study population, for various MICs (Table 10). If we define successful dosing as achieving a PTA of ≥90%, the standard cefazolin dose of 2000 mg intravenously before surgery is effective for MIC values up to 4 mg/L, except in cases of augmented eGFR.

Table 12. Probability of target attainment in simulated population with various functional renal statuses at different minimal inhibitory concentration values considering a PK/PD target of fT>MIC = 100%

MIC (mg/L)	**eGFR = 0.67-2.8 mL/s PTA (%)**	**eGFR < 2.17 mL/s**	**eGFR ≥ 2.17 mL/s PTA (%)**
0.25	99.7	99.8	97.9
0.5	99.5	99.5	96.1
1	98.8	99.0	92.4
1.5	98.1	98.3	88.7
2	97.2	97.4	84.7
3	95.1	95.5	77.1
4	92.6	93.1	69.7

Abbreviations: eGFR = glomerular filtration rate estimated according to CKD-EPI formula; MIC = minimal inhibitory concentration

Discussion

In the first part of this thesis, the influence of different modalities on the PK of drugs in pediatric and neonatal populations (appendices 1-3) was discussed.

The influence of ECMO on the PK of drugs is a complex and multifaceted phenomenon and depends on several factors (44, 45). It highly varies between different drugs, and even individual patient responses may differ. Therefore, it is essential to study the PK of individual drugs during ECMO to establish optimal dosing recommendations for patients undergoing ECMO. In this thesis, the impact of ECMO on PK of phenobarbital and meropenem in neonatal and pediatric population was described. In neonates, ECMO was found to rapidly increase CL of phenobarbital, whereas changes in phenobarbital's Vd were not identified. CL increased linearly with time during ECMO. However, ECMO did not induce any changes in PK of meropenem in pediatric and neonatal population.

Previous studies reported an increase in Vd during neonatal ECMO, typically attributed to factors such as hemodilution from circuit priming and systemic inflammatory responses causing capillary leakage and fluid retention (44, 46). These changes in Vd usually occur rapidly at the initiation of ECMO and then stabilize. It is plausible that the limited data collection at early time points after ECMO initiation in our studies hindered the detection of potential alterations in Vd of phenobarbital and meropenem.

Regarding CL, previous publications have reported increase, decrease or no changes induced by ECMO (44, 47). The increase in CL values during ECMO may be influenced by factors beyond improved organ perfusion and oxygenation. Firstly, the transit of blood through the ECMO circuit can lead to the degradation or sequestration of administered drugs (48). Sequestration in ECMO circuits is unpredictable and depends on various factors, with lipophilic drugs being more prone to sequestration than hydrophilic ones (48, 49). Additionally, sequestration may be higher with increased plasma protein binding. Phenobarbital, with a log P of 1.47 and 25–40% protein binding, might show moderate sequestration, whereas meropenem with a logP of -4.4 and protein binding of 2% is expected to show very low sequestration (50). This could be an explanation why ECMO induced increase of CL and did not influence CL of meropenem on the other hand.

According to the final model, CL increased more than 3 times during 12 days of ECMO. This anticipated increase is expected to eventually achieve a plateau, but this was not noted throughout the current study's duration. A similar phenomenon was reported by Kleiber et al. (51) in a pediatric population receiving ECMO, specifically noting a time-dependent increase in clonidine CL with a sigmoidal function reaching maximum CL around 18–20 days into ECMO treatment. Since the individuals in this analysis were treated for a maximum of 12 days, the duration may have been too short to observe the plateau in maximum CL increase. Therefore, findings from this study should not be extrapolated to period beyond the 12-day ECMO treatment.

Patients on ECMO are critically ill patients, and very often require use of CRRT, which can also have significant but variable effects on both CL and Vd of drugs (52). CRRT was found to increase Vd of

meropenem two times, whereas no influence of CRRT was found on the PK of phenobarbital. Regarding phenobarbital, only one recent study tested CRRT as a covariate on phenobarbital PK. This study found that continuous VV hemodiafiltration (CVVHDF), a form of CRRT, increased CL of phenobarbital 6 times (53). The difference in results between our study and the referenced one can be attributed to the limited number of patients undergoing CRRT in our study, with only one patient in this category. The impact of CRRT on the PK of meropenem in critically ill pediatric patients has generated varied and debated findings. Our study aligns with a prior investigation into meropenem PK in critically ill children, revealing a 66% increase in Vd associated with CRRT (54). This elevation in Vd could be ascribed to fluid overload commonly observed in patients undergoing CRRT, particularly affecting hydrophilic drugs like meropenem (52). In contrast, studies by Wang et al. (55) and Tan et al. (56) found that CRRT did not significantly impact either meropenem Vd or CL. Nevertheless, a recent study by Thy et al. (57) discovered that the total effluent flow (one of the CRRT parameters) influenced CL in critically ill children.

To highlight the practical implications of our model for phenobarbital dosing in neonates on ECMO, model-based simulations were performed. The median and 95% prediction interval of simulated concentrations were compared with target concentrations for neonatal seizures (15–40 mg/L), as specific therapeutic concentrations for sedation and neuroprotection are yet to be established (36). The results suggest that the current recommended MD (5 mg/kg/day for neonates of PNA = 0–14 d and 6 mg/kg/d for neonates of PNA = 15–28 d) may not be suitable for older neonates or those undergoing ECMO for an extended period. The model proposes, and simulations support, a more optimal dosing regimen, starting with a MD of 4 mg/kg/day that increases by 0.25 mg/kg every 12 hours during ECMO treatment. Furthermore, considering the substantial variability in the PK of phenobarbital in neonates on ECMO (as illustrated in Figure 5), not all patients may receive optimal treatment with the model-derived regimen. Some portions of the 95% prediction interval for simulated concentrations fall outside the therapeutic range. Consequently, TDM should still be considered on a case-by-case basis, even with the regimen derived from the model.

Based on Monte Carlo simulations, for meropenem-susceptible pathogens with MICs below 0.5 mg/L, suitable for meropenem monotherapy, all patients achieved a high probability of PTA at concentrations exceeding 40% of the dosing interval (fT40% > MIC). This was achieved with i.v. meropenem administration at either 20–40 mg/kg over a 3-hour prolonged infusion three times daily or continuous infusion with 60 or 120 mg/kg/day. However, for susceptible pathogens with 100% fT > MIC and MICs over 0.5 mg/L, no regimen achieved a high PTA for 100% fT > MIC. In the "grey zone" of pathogens with MICs between 2-8 mg/L, where higher meropenem doses or combination antibiotic treatment is often recommended, simulations showed the following: PTA for 40% fT > MIC was achieved for MIC up to 4 mg/L across all weight categories, treatment modalities, and dosing regimens of meropenem, except for SI of 20 - 40 mg/kg over 30 minutes in patients not undergoing CRRT. However, no dosing regimen achieved PTA at 100% fT > MIC, with a slightly higher success rate in ECMO patients with CRRT compared to those without CRRT.

In addition to ECMO modality, we have tested the effect of therapeutic hypothermia on PK of phenobarbital in asphyxiated neonates with HIE (appendix 2). The obtained results of PK parameters in this study were compared with the results of the studies evaluating phenobarbital PK in the past 20 years (32, 37-43) in Table 3. Directly comparing findings across studies is challenging due to differences in parameterization. To allow comparison, PK parameters were calculated for the typical individual in our current study, with a BW of 3.3 kg and PNA of 2 days, using equations from the referenced publications. The Vd for our typical individual aligns with values reported in most previous studies. Although reported CL values exhibit higher variability, the CL value obtained in our study does fall within the reported range. Table 3 does not imply that reported differences are caused by use of therapeutic hypothermia treatment, a conclusion consistent with prior studies (37, 38). Additionally, it also does not indicate that severity of asphyxia and severity of HIE influence PK of phenobarbital. Discrepancies could be attributed to variations in data analysis approaches, as a population approaches with separate quantification of RUV and IIV tend to yield less biased estimates (58). Additionally, systematic covariate analysis may mitigate confounding factors related to maturation and disease severity. Variability in age and BW across studies may also influence parameter estimates, particularly when the typical individual represents a child at the lower extreme of the age and weight range. Lastly, differences in administration routes could result in divergent estimates, especially in the absence of intravenous data, where bioavailability cannot be quantified, leading to parameter values reflecting reported over bioavailability. This implies that the true parameter value deviates proportionally from the apparent value based on bioavailability.

The second part of this thesis discussed the impact of different therapeutic modalities on the PK of drugs in adult population (appendices 4-7).

The three principal treatment options for patients with ESRD are hemodialysis, peritoneal dialysis, and kidney transplantation (59). ESRD patients receiving hemodialysis often require multiple medications to manage both their underlying condition and complications arising during extended hemodialysis sessions (60). A significant number of these medications are dialyzable, and the elimination of these drugs during hemodialysis may impact their therapeutic effectiveness if adequate supplementary doses are not administered. Peritoneal dialysis serves as an alternative RRT for patients with chronic end-stage renal failure, contributing to an enhanced quality of life. However, the risk of infection and inflammation of the peritoneal membrane, primarily associated with the permanent catheter, poses significant clinical challenges for patients receiving peritoneal dialysis (61). In addition to antibiotics for treating infectious peritonitis, various drugs are commonly prescribed to address attendant complications. Given the impact of peritoneal dialysis on the systemic CL of drugs is not negligible, understanding the PK of medications in these patients is crucial for making rational dosing adjustments (62).

We have described PK of vancomycin in ESRD patients receiving peritoneal dialysis (appendix 4). Our analysis revealed that the preservation of diuresis and eGFR were the primary factors influencing

vancomycin CL, while BW served as a significant covariate for Vd. Additionally, simulations based on the model suggested that the existing dosing recommendations by the ISPD fail to achieve the desired drug exposure targets in the peritoneal cavity for the majority of patients with preserved diuresis (see Figure 16). Therefore, we proposed a new vancomycin regimen, consisting of utilizing the minimum recommended i.p. LD of 20 mg/L for a continuous dosing regimen, followed by MD of 50 mg/L for each dwell (Figure 17). This strategy ensures adequate exposure within the peritoneum from the initiation of treatment. Due to variations in peritoneal membrane permeability during different peritonitis occurrences, predicting plasma levels can be challenging. Therefore, we recommend monitoring plasma levels no later than the fifth day of treatment to adjust dosing in patients at risk of excessive systemic exposure. Subsequent monitoring should be conducted regularly, as levels may steadily increase in some patients due to slow vancomycin accumulation, particularly in cases of markedly prolonged elimination half-life. Oliguric patients may require dose reduction if plasma levels exceed 25 mg/L. Our recommended dosing strategy aims to maximize peritoneal exposure, ensuring that the AUC_{24} consistently surpasses the target values recommended by Rybak for systemic levels (27). While concerns about potentially unnecessary high peritoneal levels may arise, the reduced efficacy of vancomycin in glucose and icodextrin-containing peritoneal dialysates, as demonstrated in our *ex vivo* samples (see Table 3 in the corresponding publication, appendix 4) and supported by previous research (63), justifies the need for higher AUC in intraperitoneal vancomycin during continuous dosing. The ineffectiveness of intermittent vancomycin administration reinforces the shift towards continuous dosing. Localized high vancomycin exposure in the peritoneum, without excessive plasma levels, poses minimal risk for systemic toxicity. Therefore, our recommendation advocates dosing vancomycin to achieve the highest feasible i.p. exposure, limited only by the risk of systemic toxicity when plasma levels surpass the recommended threshold.

Another important aspect of our study is that we confirmed clinically relevant IOV in peritoneal membrane permeability for vancomycin during different episodes of peritonitis (Figure 11). This variability adds a clinical challenge to the prediction of plasma levels, likely attributed to differences in the severity of peritoneal membrane inflammation during specific peritonitis episodes. The poor correlation between trough plasma vancomycin concentrations and treatment effectiveness observed in other studies may be attributed to this variability, as these levels also inadequately correlate with i.p. levels (64, 65).

We have also described PK of fondaparinux in one ESDR patient undergoing peritoneal dialysis, in addition to those patients undergoing HF and LF hemodialysis (appendix 5). Our analysis revealed that LF membranes did not elevate the CL of fondaparinux. This is in line with expectations given the molecular size of fondaparinux (1.7 kDa), which surpasses the threshold for LF membrane filtration. Conversely, HF membranes are anticipated to more effectively eliminate fondaparinux. Our analysis showed that CL during HF dialysis is 2.26 times higher than CL during LF hemodialysis. HF membranes exhibited a less substantial increase in CL than initially expected. This could be

attributed to the high affinity of fondaparinux for antithrombin III, resulting in over 97% binding in plasma, impeding the dialysis of fondaparinux (66). Additionally, this study was the first to discuss PK of fondaparinux in a patient receiving peritoneal dialysis. The jackknife analysis, along with GOF plots and individual parameter values, indicates that the outcomes observed for patients with LF membranes and those not undergoing hemodialysis may extend to ESRD individuals undergoing peritoneal dialysis. However, larger study cohorts are essential to corroborate these findings for the latter patient group.

In our laboratory, the lab-specific correlation between anti-Xa activity and fondaparinux plasma concentrations was 1.18 (r^2 = 0.97). While this value was fixed and not estimated in our PK-PD analysis, we did estimate an IIV on this parameter. The IIV was found to be relatively low at 13.9%, but due to its low reliability, it was not retained in the final model. Covariate effects were only tested on PK parameters.

Simulations were performed to illustrate our findings. Target anti-Xa levels are still not established, so we have compared median and 95% of predicted anti-Xa activity with previously published activities (these are given in Table 3 in the corresponding publication, appendix 5). According to the available literature, as well as our clinical empirical experience, anti-Xa activity before and after dialysis should be approximately 0.3 IU/mL, and in the range 0.5–1 IU/mL, respectively. In our study, steady-state pre-dialysis levels were 0.4 and 0.55 IU/mL for HF and LF hemodialysis, respectively, and steady-state post-dialysis levels were 0.72 and 0.98 IU/mL for HF and LF hemodialysis, respectively. Figure 20 illustrates the variability in anti-Xa activity among ESRD patients undergoing hemodialysis, represented by a 95% prediction interval. This interval exhibits a roughly fourfold difference between the lowest and highest values, a pattern consistent with observations in other clinical studies (67-71). The figure emphasizes that, even with clinically feasible dosing, anti-Xa concentrations in some patients may fall outside the target range defined in the study. While the clinical impact of anti-Xa levels beyond the target range is unclear, the option of TDM could be considered to assess individual patients' anti-Xa levels if necessary. Furthermore, simulations suggest that an initial loading dose of 5 mg is recommended for achieving steady-state anti-Xa activity levels and ensuring fully effective anticoagulation right from the start of treatment.

We have also analyzed the PK of ampicillin and cefazolin in patients undergoing cardiac operation with ECC (appendices 6 and 7). Similarly to ECMO, ECC can induce significant PK and PD changes, due to sequestration of drugs and albumin on the ECC tubing, and hemodilution caused by the priming of the drug, inflammatory response and water retention (72). Currently, there are two main ECC systems: conventional ECC, and MiECC, which has been developed to minimize the biological impact of ECC, resulting in less interaction with drugs (73).

We have revealed that conventional ECC had no impact of ECC on ampicillin PK. On another hand, our analysis found both ECC and MiECC decrease peripheral Vd, while BSA and eGFR were identified as significant covariates of central Vd and CL, respectively.

For ampicillin, Monte Carlo simulations were performed and time to achieve PTA>95% for various PK/PD targets (50% and 100%fT>MIC), for different MIC values and different eGFR values. For patients receiving ampicillin prophylactically, it is assumed that PK/PD target for 50% fT>MIC would be sufficient. For these patients, for MIC = 8 mg/L, dose of 2000 mg of ampicillin administered before the surgery is not sufficient if the CBP operation lasts longer than 430 min, 320 min, 220 min and 140 min in patients with moderate to severe renal impairment, in patients with mild renal impairment, in patients with normal renal function and in patients with an increased eGFR, respectively. In that case, an additional dose (1000 mg i.v.) should be administered.

For cefazolin, Monte Carlo simulations were used to predict PTA during 407 min, as this was the length of cefazolin administration. Simulations were performed for patients with various functional renal statuses (eGFR < 1 mL/s, 1–2.17 mL/s and >2.17 mL/s) in the distribution corresponding to the real study population, for various MICs. If we define successful dosing as achieving a PTA of ≥90%, the standard cefazolin dose of 2000 mg intravenously before surgery is effective for MIC values up to 4 mg/L, except in cases of augmented eGFR.

Conclusions

The topic of this thesis was to describe the PK of various drugs in various therapeutic modalities in neonatal, pediatric and adult population. The conclusions of the thesis are following:

- In neonates, ECMO was found to rapidly increase CL of phenobarbital, whereas changes in phenobarbital's Vd were not identified. CL increased linearly with time during ECMO. This trend resulted in a continuous decline in phenobarbital exposure, heightening the risk of therapeutic failure over time. The desired target levels are reached within the initial 12 days of ECMO when employing a regimen comprising an LD of 20 mg/kg and MD of 4 mg/kg/day, divided into two doses, with an increase of 0.25 mg/kg every 12 hours throughout the ECMO treatment period. Given the substantial unexplained PK variability in this population, it is advisable to implement frequent and repeated TDM, even when using the regimen derived from the model.
- In neonatal and pediatric patients, ECMO did not induce any changes in the PK of meropenem in pediatric and neonatal population. Additionally, BW emerged as a significant covariate for both CL and Vd. Lastly, Vd exhibited an approximately twofold increase in patients undergoing CRRT. Monte Carlo simulations showed that most of currently recommended dosing regimens achieved high probability of PTA for MICs up to 4 mg/L across all BW categories and treatment modalities (both CRRT on and off) for 40% fT > MIC, but not for 100% fT > MIC.
- Therapeutic hypothermia, in addition to severity of asphyxia and severity of HIE, did not influence the PK of phenobarbital in asphyxiated neonates with HIE. BW was found to be the only significant covariate for the Vd of phenobarbital. No adjustments of dosing of phenobarbital were proposed for this population.
- In ESRD patients in patients undergoing peritoneal dialysis, the preservation of diuresis and eGFR were the primary factors influencing vancomycin CL, while BW served as a significant covariate for Vd of vancomycin. Additionally, simulations based on the model suggested that the existing dosing recommendations fail to achieve the desired drug exposure targets in the peritoneal cavity for the majority of patients with preserved diuresis. A new dosing regimen was proposed, consisting of i.p. LD of 20 mg/L for a continuous dosing regimen, followed by MD of 50 mg/L for each dwell.
- In ESRD patients, fondaparinux CL during HF hemodialysis increased 2.26 times, whereas LF hemodialysis and peritoneal dialysis did not affect CL of fondaparinux. Model-based simulations suggested that an initial LD of 5 mg should be recommended for achieving steady-state anti-Xa activity levels, ensuring fully effective anticoagulation right from the start of treatment.
- In patients undergoing cardiac operation, there was no impact of ECC on ampicillin PK. EGFR was found to be a significant covariate for ampicillin CL, and BW served as predictive covariate for both V1 and V2. According to simulations, for 50% fT>MIC, for MIC = 8 mg/L, dose of 2000 mg of ampicillin administered before the surgery is not sufficient if the

operation lasts longer than 430 min, 320 min, 220 min and 140 min in patients with moderate to severe renal impairment, in patients with mild renal impairment, in patients with normal renal function and in patients with an increased eGFR, respectively. In these cases, an additional dose (1000 mg i.v.) should be administered.

- Both standard ECC and MiECC were found to decrease cefazolin peripheral Vd, while BSA and eGFR were identified as significant covariates of central Vd and CL, respectively. Simulations showed that the standard cefazolin dose of 2000 mg i.v. before surgery was effective for MIC values up to 4 mg/L, except in cases of augmented eGFR.

References

1. Reynolds, J.L. and M.T. Rupp, *Improving clinical decision support in pharmacy: toward the perfect DUR alert.* Journal of managed care & specialty pharmacy, 2017. **23**(1): p. 38-43.
2. Usman, M., et al., *Pharmacometrics: A New Era of Pharmacotherapy and Drug Development in Low- and Middle-Income Countries.* Advances in Pharmacological and Pharmaceutical Sciences, 2023. **2023**.
3. Awaisu, A. and T. Chen, *Encyclopedia of Pharmacy Practice and: Clinical Pharmacy*. 2019: Elsevier.
4. Barrett, J.S., et al., *Pharmacometrics: a multidisciplinary field to facilitate critical thinking in drug development and translational research settings.* The Journal of Clinical Pharmacology, 2008. **48**(5): p. 632-649.
5. Chan Kwong, A.H.-X.P., et al., *Prior information for population pharmacokinetic and pharmacokinetic/pharmacodynamic analysis: overview and guidance with a focus on the NONMEM PRIOR subroutine.* Journal of pharmacokinetics and pharmacodynamics, 2020. **47**: p. 431-446.
6. De Cock, R.F., et al., *The role of population PK–PD modelling in paediatric clinical research.* European journal of clinical pharmacology, 2011. **67**: p. 5-16.
7. Dallmann, A., et al., *Applied concepts in PBPK modeling: how to extend an open systems pharmacology model to the special population of pregnant women.* CPT: pharmacometrics & systems pharmacology, 2018. **7**(7): p. 419-431.
8. Kuepfer, L., et al., *Applied concepts in PBPK modeling: how to build a PBPK/PD model.* CPT: pharmacometrics & systems pharmacology, 2016. **5**(10): p. 516-531.
9. Ette, E.I., P.J. Williams, and J.R. Lane, *Population pharmacokinetics III: design, analysis, and application of population pharmacokinetic studies.* Annals of Pharmacotherapy, 2004. **38**(12): p. 2136-2144.
10. Mould, D.R. and R. Upton, *Basic concepts in population modeling, simulation, and model-based drug development.* CPT: pharmacometrics & systems pharmacology, 2012. **1**(9): p. 1-14.
11. Mould, D.R. and R.N. Upton, *Basic concepts in population modeling, simulation, and model-based drug development—part 2: introduction to pharmacokinetic modeling methods.* CPT: pharmacometrics & systems pharmacology, 2013. **2**(4): p. 1-14.
12. Wade, J.R., S.L. Beal, and N.C. Sambol, *Interaction between structural, statistical, and covariate models in population pharmacokinetic analysis.* Journal of pharmacokinetics and biopharmaceutics, 1994. **22**(2): p. 165-177.
13. Boeckmann, A.J., L.B. Sheiner, and S.L. Beal, *NONMEM users guide-part V: introductory guide.* NONMEM Project Group. University of California at San Francisco, 1994.
14. Sheiner, L.B. and T. Ludden, *Population pharmacokinetics/dynamics.* Annual review of pharmacology and toxicology, 1992. **32**(1): p. 185-209.
15. Box, G.E. and N.R. Draper, *Empirical model-building and response surfaces*. 1987: John Wiley & Sons.
16. Sun, H., et al., *Population pharmacokinetics: a regulatory perspective.* Clinical pharmacokinetics, 1999. **37**: p. 41-58.
17. Hooker, A.C., C.E. Staatz, and M.O. Karlsson, *Conditional weighted residuals (CWRES): a model diagnostic for the FOCE method.* Pharmaceutical research, 2007. **24**: p. 2187-2197.
18. Sherwin, C.M., et al., *Fundamentals of population pharmacokinetic modelling: validation methods.* Clinical pharmacokinetics, 2012. **51**: p. 573-590.
19. Comets, E., K. Brendel, and F. Mentré, *Computing normalised prediction distribution errors to evaluate nonlinear mixed-effect models: the npde add-on package for R.* Computer methods and programs in biomedicine, 2008. **90**(2): p. 154-166.
20. Kearns, G.L., et al., *Developmental pharmacology—drug disposition, action, and therapy in infants and children.* New England Journal of Medicine, 2003. **349**(12): p. 1157-1167.

21. Grand, R.J., J.B. Watkins, and F.M. Torti, *Development of the human gastrointestinal tract: a review.* Gastroenterology, 1976. **70**(5): p. 790-810.
22. de Wildt, S.N., et al., *Glucuronidation in humans: pharmacogenetic and developmental aspects.* Clinical pharmacokinetics, 1999. **36**: p. 439-452.
23. Hines, R.N. and D.G. McCarver, *The ontogeny of human drug-metabolizing enzymes: phase I oxidative enzymes.* Journal of Pharmacology and Experimental Therapeutics, 2002. **300**(2): p. 355-360.
24. Rhodin, M.M., et al., *Human renal function maturation: a quantitative description using weight and postmenstrual age.* Pediatric nephrology, 2009. **24**: p. 67-76.
25. Bartelink, I.H., et al., *Guidelines on paediatric dosing on the basis of developmental physiology and pharmacokinetic considerations.* Clinical pharmacokinetics, 2006. **45**: p. 1077-1097.
26. Li, P.K.-T., et al., *ISPD peritonitis guideline recommendations: 2022 update on prevention and treatment.* Peritoneal Dialysis International, 2022. **42**(2): p. 110-153.
27. Rybak, M.J., et al., *Therapeutic monitoring of vancomycin for serious methicillin-resistant Staphylococcus aureus infections: a revised consensus guideline and review by the American Society of Health-System Pharmacists, the Infectious Diseases Society of America, the Pediatric Infectious Diseases Society, and the Society of Infectious Diseases Pharmacists.* American Journal of Health-System Pharmacy, 2020. **77**(11): p. 835-864.
28. Lindbom, L., P. Pihlgren, and N. Jonsson, *PsN-Toolkit—a collection of computer intensive statistical methods for non-linear mixed effect modeling using NONMEM.* Computer methods and programs in biomedicine, 2005. **79**(3): p. 241-257.
29. Lindbom, L., J. Ribbing, and E.N. Jonsson, *Perl-speaks-NONMEM (PsN)—a Perl module for NONMEM related programming.* Computer methods and programs in biomedicine, 2004. **75**(2): p. 85-94.
30. Keizer, R.J., et al., *Pirana and PCluster: a modeling environment and cluster infrastructure for NONMEM.* Computer methods and programs in biomedicine, 2011. **101**(1): p. 72-79.
31. Donat, F., et al., *The pharmacokinetics of fondaparinux sodium in healthy volunteers.* Clinical pharmacokinetics, 2002. **41**: p. 1-9.
32. Völler, S., et al., *Model-based clinical dose optimization for phenobarbital in neonates: an illustration of the importance of data sharing and external validation.* European Journal of Pharmaceutical Sciences, 2017. **109**: p. S90-S97.
33. D'Alton, M.E., et al., *Neonatal encephalopathy and neurologic outcome.* Obstetrics and gynecology (New York. 1953), 2014. **123**(4): p. 896-901.
34. Jacobs, S., *Whole-body hypothermia for neonatal hypoxic–ischemic encephalopathy reduces mortality into childhood.* The Journal of Pediatrics, 2012. **161**(5): p. 968-969.
35. Pokorná, P., et al., *Severity of asphyxia is a covariate of phenobarbital clearance in newborns undergoing hypothermia.* The Journal of Maternal-Fetal & Neonatal Medicine, 2019. **32**(14): p. 2302-2309.
36. https://www.kinderformularium.nl/.
37. Shellhaas, R.A., et al., *Population pharmacokinetics of phenobarbital in infants with neonatal encephalopathy treated with therapeutic hypothermia.* Pediatric critical care medicine: a journal of the Society of Critical Care Medicine and the World Federation of Pediatric Intensive and Critical Care Societies, 2013. **14**(2): p. 194.
38. Van Den Broek, M., et al., *Pharmacokinetics and clinical efficacy of phenobarbital in asphyxiated newborns treated with hypothermia: a thermopharmacological approach.* Clinical pharmacokinetics, 2012. **51**: p. 671-679.
39. Filippi, L., et al., *Phenobarbital for neonatal seizures in hypoxic ischemic encephalopathy: a pharmacokinetic study during whole body hypothermia.* Epilepsia, 2011. **52**(4): p. 794-801.

40. Marsot, A., et al., *Pharmacokinetics and absolute bioavailability of phenobarbital in neonates and young infants, a population pharmacokinetic modelling approach.* Fundamental & clinical pharmacology, 2014. **28**(4): p. 465-471.
41. Moffett, B.S., et al., *Phenobarbital population pharmacokinetics across the pediatric age spectrum.* Epilepsia, 2018. **59**(7): p. 1327-1333.
42. Touw, D., et al., *Clinical pharmacokinetics of phenobarbital in neonates.* European journal of pharmaceutical sciences, 2000. **12**(2): p. 111-116.
43. Yukawa, M., et al., *Population pharmacokinetics of phenobarbital by mixed effect modelling using routine clinical pharmacokinetic data in Japanese neonates and infants: an update.* Journal of clinical pharmacy and therapeutics, 2011. **36**(6): p. 704-710.
44. Di Nardo, M. and E.D. Wildschut, *Drugs pharmacokinetics during veno-venous extracorporeal membrane oxygenation in pediatrics.* Journal of Thoracic Disease, 2018. **10**(Suppl 5): p. S642.
45. Zeilmaker, G.A., et al., *Pharmacokinetic considerations for pediatric patients receiving analgesia in the intensive care unit; targeting postoperative, ECMO and hypothermia patients.* Expert Opinion on Drug Metabolism & Toxicology, 2018. **14**(4): p. 417-428.
46. Ha, M.A. and A.C. Sieg, *Evaluation of altered drug pharmacokinetics in critically ill adults receiving extracorporeal membrane oxygenation.* Pharmacotherapy: The Journal of Human Pharmacology and Drug Therapy, 2017. **37**(2): p. 221-235.
47. Cheng, V., et al., *Optimising drug dosing in patients receiving extracorporeal membrane oxygenation.* Journal of thoracic disease, 2018. **10**(Suppl 5): p. S629.
48. Shekar, K., et al., *Protein-bound drugs are prone to sequestration in the extracorporeal membrane oxygenation circuit: results from an ex vivo study.* Critical Care, 2015. **19**: p. 1-8.
49. Shekar, K., et al., *Pharmacokinetic changes in patients receiving extracorporeal membrane oxygenation.* Journal of critical care, 2012. **27**(6): p. 741. e9-741. e18.
50. Wishart, D.S., et al., *DrugBank 5.0: a major update to the DrugBank database for 2018.* Nucleic acids research, 2018. **46**(D1): p. D1074-D1082.
51. Kleiber, N., et al., *Population pharmacokinetics of intravenous clonidine for sedation during paediatric extracorporeal membrane oxygenation and continuous venovenous hemofiltration.* British journal of clinical pharmacology, 2017. **83**(6): p. 1227-1239.
52. Jang, S.M. and L. Awdishu. *Drug dosing considerations in continuous renal replacement therapy*. in *Seminars in Dialysis*. 2021. Wiley Online Library.
53. Thibault, C., et al., *Population pharmacokinetics of phenobarbital in neonates and infants on extracorporeal membrane oxygenation and the influence of concomitant renal replacement therapy.* The Journal of Clinical Pharmacology, 2021. **61**(3): p. 378-387.
54. Saito, J., et al., *Population pharmacokinetics and pharmacodynamics of meropenem in critically ill pediatric patients.* Antimicrobial Agents and Chemotherapy, 2021. **65**(2): p. 10.1128/aac. 01909-20.
55. Wang, Y., et al., *Optimized dosing regimens of meropenem in septic children receiving extracorporeal life support.* Frontiers in Pharmacology, 2021. **12**: p. 699191.
56. Tan, W.W., et al., *Optimal dosing of meropenem in a small cohort of critically ill children receiving continuous renal replacement therapy.* The Journal of Clinical Pharmacology, 2021. **61**(6): p. 744-754.
57. Thy, M., et al., *Meropenem population pharmacokinetics and dosing regimen optimization in critically ill children receiving continuous renal replacement therapy.* Clinical Pharmacokinetics, 2022. **61**(11): p. 1609-1621.
58. Krekels, E.H., et al., *Prediction of morphine clearance in the paediatric population: how accurate are the available pharmacokinetic models?* Clinical pharmacokinetics, 2012. **51**: p. 695-709.
59. O'Shaughnessy, M.M., et al., *Differences in initial treatment modality for end-stage renal disease among glomerulonephritis subtypes in the USA.* Nephrology Dialysis Transplantation, 2016. **31**(2): p. 290-298.

60. Atkinson Jr, A. and J. Umans, *Pharmacokinetic studies in hemodialysis patients.* Clinical Pharmacology & Therapeutics, 2009. **86**(5): p. 548-552.
61. Kim, K., et al., *Pharmacokinetic profiles of ceftazidime after intravenous administration in patients undergoing automated peritoneal dialysis.* Antimicrobial agents and chemotherapy, 2011. **55**(6): p. 2523-2527.
62. Horiuchi, M., et al., *Effects of peritoneal dialysis on pharmacotherapy: a deductive pharmacokinetic-model approach to predict drug concentration profiles in plasma and peritoneal fluid.* Drug Metabolism and Pharmacokinetics, 2014. **29**(2): p. 154-161.
63. Tobudic, S., et al., *Comparative in vitro antimicrobial activity of vancomycin, teicoplanin, daptomycin and ceftobiprole in four different peritoneal dialysis fluids.* European journal of clinical microbiology & infectious diseases, 2012. **31**: p. 1327-1334.
64. Stevenson, S., et al., *The role of monitoring vancomycin levels in patients with peritoneal dialysis-associated peritonitis.* Peritoneal Dialysis International, 2015. **35**(2): p. 222-228.
65. Blunden, M., et al., *Single UK centre experience on the treatment of PD peritonitis—antibiotic levels and outcomes.* Nephrology Dialysis Transplantation, 2007. **22**(6): p. 1714-1719.
66. Paolucci, F., et al., *Fondaparinux sodium mechanism of action: identification of specific binding to purified and human plasma-derived proteins.* Clinical pharmacokinetics, 2002. **41**: p. 11-18.
67. Speeckaert, M.M., et al., *Fondaparinux as an alternative to vitamin K antagonists in haemodialysis patients.* Nephrology Dialysis Transplantation, 2013. **28**(12): p. 3090-3095.
68. Mahieu, E., et al., *Anticoagulation with fondaparinux for hemodiafiltration in patients with heparin-induced thrombocytopenia: dose-finding study and safety evaluation.* Artificial organs, 2013. **37**(5): p. 482-487.
69. Kalicki, R.M., et al., *Use of the pentasaccharide fondaparinux as an anticoagulant during haemodialysis.* Thrombosis and haemostasis, 2007. **98**(12): p. 1200-1207.
70. Ho, G., et al., *Use of fondaparinux for circuit patency in hemodialysis patients.* American journal of kidney diseases, 2013. **61**(3): p. 525-526.
71. Sombolos, K., et al., *Use of fondaparinux as an anticoagulant during hemodialysis: a preliminary study.* International journal of clinical pharmacology and therapeutics, 2008. **46**(4): p. 198-203.
72. Wahba, A., et al., *2019 EACTS/EACTA/EBCP guidelines on cardiopulmonary bypass in adult cardiac surgery.* European Journal of Cardio-Thoracic Surgery, 2020. **57**(2): p. 210-251.
73. Condello, I., et al., *Propofol pharmacokinetics and pharmacodynamics—a perspective in minimally invasive extracorporeal circulation.* Interactive Cardiovascular and Thoracic Surgery, 2021. **33**(4): p. 625-627.

Appendices

Appendix 1: Michalicková, D.*, Pokorná, P., Tibboel, D., et al. (2020). Rapid increase in clearance of phenobarbital in neonates on extracorporeal membrane oxygenation: a pilot retrospective population pharmacokinetic analysis. Pediatr Crit Care Med 21(9), e707-e715. Link: https://journals.lww.com/pccmjournal/abstract/2020/09000/rapid_increase_in_clearance_of_phenobarbital_in.37.aspx

Appendix 2: Pokorná, P., Michaličková, D.*, Völler, S., et al. (2022). Severity parameters for asphyxia or hypoxic-ischemic encephalopathy do not explain inter-individual variability in the pharmacokinetics of phenobarbital in newborns treated with therapeutic hypothermia. Minerva Pediatr 74(2), 107-115. Link: https://europepmc.org/article/med/33107271

Appendix 3: Pokorna, P., Michalickova, D.*, Tibboel, D., et al. Meropenem disposition in neonatal and pediatric extracorporeal membrane oxygenation. **Note: accepted for publication in *Antibiotics***

Appendix 4: Hartinger, J. M., Michaličková, D., Dvořáčková, E., et al. (2023). Intraperitoneally Administered Vancomycin in Patients with Peritoneal Dialysis-Associated Peritonitis: Population Pharmacokinetics and Dosing Implications. Pharmaceutics 15(5), 1394. Link: https://www.mdpi.com/1999-4923/15/5/1394

Appendix 5: Michaličková, D*., Hartinger, J. M., Hladinová, Z., et al. (2022). Population pharmacokinetics-pharmacodynamics of fondaparinux in dialysis-dependent chronic kidney disease patients undergoing chronic renal replacement therapy. Eur J Clin Pharmacol 78(1), 89-98. Link: https://link.springer.com/article/10.1007/s00228-021-03201-1

Appendix 6: Urbánek, K., Šantavý, P., Zuščich, O., Kubíčková, V., Michaličková, D., et al. (2023). Population pharmacokinetic model-based dosing proposal for ampicillin prophylaxis in cardiac surgery patients with cardiopulmonary bypass. J Chemother 35(7), 614-622. Link:

Appendix 7: Šantavý, P., Šíma, M., Zuščich, O., Kubíčková, V., Michaličková, D., et al. (2022). Population pharmacokinetics of prophylactic cefazolin in cardiac surgery with standard and minimally invasive extracorporeal circulation. Antibiotics 11(11), 1582. Link: https://www.mdpi.com/2079-6382/11/11/1582